

Supporting Information

Antimony vs bismuth: structural differences in Cat{[MCl₅](I₂)} halogen bond-linked supramolecular complexes

The choice of space group for compound 1 refinement

Initially, we solved and refined the crystal structure of compound 1 in *Pnma* space group (as in 2). This resulted in high R-factors ($R_1 = 7.16\%$, $wR_2 = 17.61\%$), poor Goodness-of-fit (1.324) and significant residual peaks without any chemical sense (max 3.081 e/Å³, min -4.066 e/Å³). All of this could be possibly an indication of twinning. No suitable twin laws were found in this space group. Also Cl atom which is in contact with I₂ molecule, was disordered which hinders possible halogen bonds evaluation. Possibility of twin refinement in less symmetrical monoclinic crystal system was made. The structure was solved and refined in space group *P2₁/n* with beta angle close to 90° (90.101°). Appropriate twin matrix (-1 0 0 0-1 0 0 0 1) was successfully found by Olex (BASF 0.41404). This resulted in much better R_1 and Goodness-of-fit (3.89% and 1.039 respectively, see data for 1 in Table S1) and absence of any disorder, which is especially good for quantum chemical calculations.

Powder X-ray diffractometry (PXRD)

Analysis of polycrystals was performed on Bruker D8 Advance (CuK α radiation, LYNXEYE XE-T linear detector, 4 – 50° 2θ range, 0.03° 2θ step, 0.5s per step). A polycrystalline sample was slightly ground with hexane in an agate mortar, and the resulting suspensions were deposited on the polished side of a standard quartz sample holder, and a smooth thin layer being formed after drying. The diffraction patterns of 1-4 were completely indexed by the results of the corresponding single crystal studies (data obtained at 150 and 220 K was used), and no extra peaks were found, which indicated that the products were a single phase.

Raman spectra were collected using a LabRAM HR Evolution (Horiba) spectrometer with the excitation by the 633 nm line of the He-Ne laser. The spectra at room temperatures were obtained in the backscattering geometry with a Raman microscope. The laser beam was focused to a diameter of 2 μm using a LMPlan FL 50x/0.50 Olympus objective. The spectral resolution was 0.7 cm⁻¹. The laser power on the sample surface was about 0.03 mW.

Differential scanning calorimetry (DSC)

Thermal analysis was performed with a NETZSCH DSC 204 F1 Phoenix differential scanning calorimeter with a digital/discrete resolution of ~0.01 μW in temperature range -153.65 °C-25 °C (120-300 K). DSC measurements were carried out by a heat flow measurement method at a 12-15 K/min cooling/heating rate in 25 mL min⁻¹ Ar flux in unsealed aluminum crucibles with lids. Powdered samples were distributed uniformly over the bottom and carefully tamped. To increase the sensitivity and reduce baseline noise, measurements were taken at a heating rate of 12-15 K/min without the supply of gas or liquid nitrogen (self-heating rate of the calorimeter cell ~10 K/min at 130 K). The sensitivity of the sample carrier sensors and temperature scale gradation were calibrated by melting and crystal to crystal transition measurements of standard samples (cyclohexane, adamantane, Hg, Ga, benzoic acid, KNO₃, In).

Thermogravimetric analysis (TGA) of 1-4 was carried out on a TG 209 F1 Iris thermobalance (NETZSCH, Germany). The measurements were made in a helium flow in the temperature range of 30-450 °C using the heating rate of 10 °C/min the gas flow rate of 60 mL/min and open Al crucibles.

Diffuse reflectance spectra of 1-4 were measured on a setup which consists of a Kolibri-2 spectrometer (VMK Optoelektronica, Russia), fiber optic cable QR-400-7 (Ocean Optics, USA), and deuterium–tungsten lamp AvaLight-DHS (Avantes, Netherlands). The reference of 100% reflectance was BaSO₄ powder. The spectra were recorded five times in the wavelength interval of 300-1000 nm and then averaged to reduce the random error.

Table S1. Crystal data and structure refinement for **1–2** and **2** at 101K.

Identification code	1	2	2_100K
CCDC number	2413116	2413117	2426309
Empirical formula	C ₁₂ H ₁₄ N ₂ SbCl ₅ I ₂	C ₁₂ H ₁₄ N ₂ BiCl ₅ I ₂	C ₁₂ H ₁₄ N ₂ BiCl ₅ I ₂
<i>M</i> , g/mol	739.05	826.28	826.28
Temperature/K	150	220	100
Crystal system	Monoclinic	Orthorhombic	Orthorhombic
Space group	<i>P</i> 2 ₁ / <i>n</i>	<i>Pnma</i>	<i>Pnma</i>
<i>a</i> , Å	14.2820 (6)	7.4735 (2)	7.3832 (4)
<i>b</i> , Å	7.3356 (3)	14.2835 (4)	14.2708 (7)
<i>c</i> , Å	19.7031 (7)	19.7322 (6)	19.6817 (9)
α , deg.	90	90	90
β , deg.	90.101 (1)	90	90
γ , deg.	90	90	90
Volume, Å ³	2064.23 (14)	2106.37 (10)	2073.75 (18)
<i>Z</i>	4	4	4
ρ_{calc} , g/cm ³	2.378	2.606	2.647
μ , mm ⁻¹	4.97	11.93	45.97
<i>F</i> (000)	1368	1496	1496
Crystal size, mm	0.14 × 0.07 × 0.05	0.25 × 0.15 × 0.03	0.06 × 0.05 × 0.02
Θ range for data collection, deg.	1.760 to 33.739	2.064 to 31.508	3.826 to 76.255
<i>T</i> _{min} , <i>T</i> _{max}	0.633, 0.747	0.166, 0.373	0.098, 0.298
Range of <i>h</i> , <i>k</i> , <i>l</i>	-22 ≤ <i>h</i> ≤ 22, -11 ≤ <i>k</i> ≤ 11, -27 ≤ <i>l</i> ≤ 30	-10 ≤ <i>h</i> ≤ 10, -21 ≤ <i>k</i> ≤ 20, -29 ≤ <i>l</i> ≤ 29	-8 ≤ <i>h</i> ≤ 9, -17 ≤ <i>k</i> ≤ 17, -23 ≤ <i>l</i> ≤ 24
(sin θ/λ) _{max} (Å ⁻¹)	0.781	0.735	0.630
<i>R</i> _{int}	0.054	0.065	0.079
No. of measured, independent and observed [<i>I</i> > 2σ(<i>I</i>)] reflections	35710, 8239, 6518	27777, 3616, 3007	13964, 2254, 2032
Data/restraints/parameters	8239/0/201	3616/100/168	2254/123/145
Goodness-of-fit on <i>F</i> ²	1.039	1.038	1.029
Final <i>R</i> indexes [<i>I</i> >=2σ(<i>I</i>)]	<i>R</i> ₁ = 0.0389, <i>wR</i> ₂ = 0.0687	<i>R</i> ₁ = 0.0268, <i>wR</i> ₂ = 0.0531	<i>R</i> ₁ = 0.0410, <i>wR</i> ₂ = 0.1041
Final <i>R</i> indexes [all data]	<i>R</i> ₁ = 0.0593, <i>wR</i> ₂ = 0.0743	<i>R</i> ₁ = 0.0379, <i>wR</i> ₂ = 0.0565	<i>R</i> ₁ = 0.0459, <i>wR</i> ₂ = 0.1083
Weighting scheme	$w = 1/[\sigma^2(F_o^2) + (0.0087P)^2 + 7.7987P]$ where $P = (F_o^2 + 2F_c^2)/3$	$w = 1/[\sigma^2(F_o^2) + (0.0179P)^2 + 0.652P]$ where $P = (F_o^2 + 2F_c^2)/3$	$w = 1/[\sigma^2(F_o^2) + (0.0597P)^2 + 4.5187P]$ where $P = (F_o^2 + 2F_c^2)/3$
(Δ/σ) _{max}	0.002	0.001	< 0.001
Largest diff. peak/hole, e/Å ³	1.80, -1.86	1.02, -0.63	3.51, -1.79
Extinction coefficient	0.00041(5)	0.00195 (8)	-

Computer programs: SHELXT 2014/5 (Sheldrick, 2014), SHELXL 2017/1 (Sheldrick, 2015), Olex2 1.5 (Dolomanov et al., 2009).

Table S2. Crystal data and structure refinement for **3**, **3_300K** and **4**.

Identification code	3	3_300K	4
CCDC number	2413118	2426310	2413119
Empirical formula	C ₁₃ H ₁₆ N ₂ Cl ₅ SbI ₂	C ₁₃ H ₁₆ N ₂ Cl ₅ SbI ₂	C ₁₃ H ₁₆ N ₂ BiCl ₅ I ₂
<i>M</i> , g/mol	753.08	753.08	840.31
Temperature/K	220	300	150
Crystal system	Orthorhombic	Orthorhombic	Monoclinic
Space group	<i>Pnma</i>	<i>Pnma</i>	<i>P2₁/c</i>
<i>a</i> , Å	15.3188 (4)	15.3811 (12)	14.3756 (3)
<i>b</i> , Å	14.2431 (3)	14.2816 (11)	18.7195 (4)
<i>c</i> , Å	9.9383 (3)	9.9869 (7)	8.2348 (2)
α , deg.	90	90	90
β , deg.	90	90	97.212 (1)
γ , deg.	90	90	90
Volume, Å ³	2168.41 (10)	2193.8 (3)	2198.49 (8)
<i>Z</i>	4	4	4
ρ_{calc} , g/cm ³	2.307	2.280	2.539
μ , mm ⁻¹	4.74	37.67	11.44
<i>F</i> (000)	1400	1400	1528
Crystal size, mm	0.22 × 0.15 × 0.06	0.09 × 0.06 × 0.06	0.18 × 0.12 × 0.02
Θ range for data collection, deg.	2.443 to 31.511	5.281 to 77.933	1.428 to 30.529
<i>T</i> _{min} , <i>T</i> _{max}	0.527, 0.746	0.089, 0.217	0.416, 0.746
Range of <i>h</i> , <i>k</i> , <i>l</i>	-20 ≤ <i>h</i> ≤ 22, -20 ≤ <i>k</i> ≤ 20, -14 ≤ <i>l</i> ≤ 14	-18 ≤ <i>h</i> ≤ 19, -16 ≤ <i>k</i> ≤ 18, -12 ≤ <i>l</i> ≤ 12	-20 ≤ <i>h</i> ≤ 20, -26 ≤ <i>k</i> ≤ 26, -11 ≤ <i>l</i> ≤ 11
(sin θ/λ) _{max} (Å ⁻¹)	0.735	0.634	0.715
<i>R</i> _{int}	0.042	0.048	0.057
No. of measured, independent and observed [<i>I</i> > 2σ(<i>I</i>)] reflections	29013, 3744, 3053	12734, 2398, 2047	28700, 6720, 5371
Data/restraints/parameters	3744/0/113	2398/0/113	6720/0/209
Goodness-of-fit on <i>F</i> ²	1.039	1.033	1.029
Final <i>R</i> indexes [<i>I</i> >=2σ(<i>I</i>)]	<i>R</i> ₁ = 0.0257, <i>wR</i> ₂ = 0.0478	<i>R</i> ₁ = 0.0288, <i>wR</i> ₂ = 0.0701	<i>R</i> ₁ = 0.0343, <i>wR</i> ₂ = 0.0611
Final <i>R</i> indexes [all data]	<i>R</i> ₁ = 0.0378, <i>wR</i> ₂ = 0.0509	<i>R</i> ₁ = 0.0348, <i>wR</i> ₂ = 0.0733	<i>R</i> ₁ = 0.0510, <i>wR</i> ₂ = 0.0651
Weighting scheme	$w = 1/[\sigma^2(F_o^2) + (0.0134P)^2 + 1.8679P]$ where <i>P</i> = (<i>F</i> _o ² + 2 <i>F</i> _c ²)/3	$w = 1/[\sigma^2(F_o^2) + (0.0328P)^2 + 0.7315P]$ where <i>P</i> = (<i>F</i> _o ² + 2 <i>F</i> _c ²)/3	$w = 1/[\sigma^2(F_o^2) + (0.0169P)^2 + 2.2265P]$ where <i>P</i> = (<i>F</i> _o ² + 2 <i>F</i> _c ²)/3
(Δ/σ) _{max}	0.002	0.001	0.003
Largest diff. peak/hole, e/Å ³	0.66, -0.74	0.47, -0.60	1.82, -0.91
Extinction coefficient	0.00187(8)	0.00034 (3)	0.00037 (4)

Computer programs: SHELXT 2014/5 (Sheldrick, 2014), SHELXL 2017/1 (Sheldrick, 2015), Olex2 1.5 (Dolomanov et al., 2009).

Table S3. Selected bond lengths and angles for **1**.

Bond length, Å			
Sb1—Cl3	2.5435 (9)	Sb1—Cl4	2.4577 (13)
Sb1—Cl2	2.4234 (9)	I1—I2	2.7453 (4)
Sb1—Cl5	2.7461 (11)	I1—Cl1	2.8121 (15)
Bond angle, (°)			
Cl3—Sb1—Cl5	175.48 (6)	Cl4—Sb1—Cl3	87.73 (6)
Cl2—Sb1—Cl3	93.19 (3)	Cl4—Sb1—Cl5	88.14 (6)
Cl2—Sb1—Cl5	85.03 (3)	I2—I1—Cl1	178.99 (4)
Cl2—Sb1—Cl4	90.58 (6)		

Symmetry code(s): (i) $-x+3/2, y-1/2, -z+3/2$; (ii) $x+1, y-1, z$.

Table S4. Selected hydrogen bond parameters for **1**.

D—H···A	D—H (Å)	H···A (Å)	D···A (Å)	D—H···A (°)
N1—H1···Cl5 ⁱ	0.88	2.57	3.258 (5)	136.1
N2—H2···Cl2 ⁱⁱ	0.88	2.86	3.495 (6)	130.8
N2—H2···Cl3 ⁱⁱⁱ	0.88	2.54	3.217 (6)	134.3
C5—H5···Cl1 ^{iv}	0.95	2.78	3.673 (8)	156.4
C6—H6A···Cl2 ^v	0.99	2.73	3.627 (5)	150.9
C6—H6B···Cl3 ^v	0.99	2.80	3.632 (5)	141.8
C11—H11···Cl4 ^{vi}	0.95	2.84	3.575 (8)	134.8
C11—H11···Cl5 ⁱⁱ	0.95	2.92	3.498 (7)	120.6

Symmetry code(s): (i) $x, y-1, z$; (ii) $x+1, y-1, z$; (iii) $x+1, y, z$; (iv) $-x+1/2, y-1/2, -z+3/2$; (v) $-x+1, -y+1, -z+1$; (vi) $-x+3/2, y-1/2, -z+3/2$.

Table S5. Selected bond lengths and angles for **2**.

Bond lengths, Å			
Bi1—Cl2	2.5999 (11)	Bi1—Cl1B ⁱⁱ	2.856 (11)
Bi1—Cl3	2.5701 (10)	Bi1—Cl1B ⁱⁱⁱ	2.856 (11)
Bi1—Cl4	2.6898 (10)	Bi1—Cl1B	2.842 (11)
Bi1—Cl4 ⁱ	2.6898 (10)	Bi1—Cl1B ⁱ	2.842 (11)
Bi1—Cl1A	2.856 (6)		
Bond angles, (°)			
Cl2—Bi1—Cl4	87.89 (2)	Cl4 ⁱ —Bi1—Cl1A ⁱⁱ	92.00 (2)
Cl2—Bi1—Cl4 ⁱ	87.89 (2)	Cl4—Bi1—Cl1A ⁱⁱ	92.00 (2)
Cl2—Bi1—Cl1A	179.3 (3)	Cl4—Bi1—Cl1A	92.09 (2)
Cl2—Bi1—Cl1A ⁱⁱ	98.1 (3)	Cl4 ⁱ —Bi1—Cl1B ⁱⁱ	87.2 (4)
Cl2—Bi1—Cl1B ⁱⁱⁱ	89.0 (13)	Cl4—Bi1—Cl1B ⁱⁱⁱ	87.2 (4)
Cl2—Bi1—Cl1B ⁱⁱ	89.0 (13)	Cl4 ⁱ —Bi1—Cl1B ⁱⁱⁱ	96.1 (4)
Cl2—Bi1—Cl1B	170.3 (12)	Cl4—Bi1—Cl1B ⁱⁱ	96.1 (4)
Cl2—Bi1—Cl1B ⁱ	170.3 (12)	Cl4 ⁱ —Bi1—Cl1B	87.9 (4)
Cl3—Bi1—Cl2	96.18 (4)	Cl4—Bi1—Cl1B ⁱ	87.9 (4)
Cl3—Bi1—Cl4	88.52 (2)	Cl4—Bi1—Cl1B	96.8 (4)
Cl3—Bi1—Cl4 ⁱ	88.52 (2)	Cl4 ⁱ —Bi1—Cl1B ⁱ	96.8 (4)
Cl3—Bi1—Cl1A ⁱⁱ	165.7 (3)	Cl1A—Bi1—Cl1A ⁱⁱ	82.58 (5)
Cl3—Bi1—Cl1A	83.2 (3)	Cl1A—Bi1—Cl1B ⁱⁱ	91.6 (11)
Cl3—Bi1—Cl1B	92.5 (13)	Cl1A—Bi1—Cl1B ⁱⁱⁱ	91.6 (11)
Cl3—Bi1—Cl1B ⁱⁱ	173.1 (11)	Cl1B ⁱ —Bi1—Cl1B ⁱⁱⁱ	82.01 (6)
Cl3—Bi1—Cl1B ⁱ	92.5 (13)	Cl1B ⁱ —Bi1—Cl1B	9.0 (9)
Cl3—Bi1—Cl1B ⁱⁱⁱ	173.1 (11)	Cl1B—Bi1—Cl1B ⁱⁱⁱ	82.71 (8)
Cl4—Bi1—Cl4 ⁱ	174.56 (5)	Bi1—Cl1A—Bi1 ^{iv}	158.2 (6)
Cl4 ⁱ —Bi1—Cl1A	92.09 (2)		

Symmetry code(s): (i) $x, -y+3/2, z$; (ii) $x-1/2, y, -z-1/2$; (iii) $x-1/2, -y+3/2, -z-1/2$; (iv) $x+1/2, y, -z-1/2$.

Table S6. Selected hydrogen bond parameters for **2**.

D—H···A	D—H (Å)	H···A (Å)	D···A (Å)	D—H···A (°)
C5—H5···Cl4 ⁱ	0.94	2.68	3.590 (11)	161.9
N2—H2A···Cl2 ⁱⁱ	0.87	2.55	3.211 (10)	133.6
N2—H2A···Cl3 ⁱⁱⁱ	0.87	2.66	3.327 (10)	133.9
C11—H11···Cl4 ^{iv}	0.94	3.06	3.720 (8)	128.4
C12—H12···Cl4 ^{iv}	0.94	3.11	3.743 (6)	126.3
C6—H6A···Cl3	0.98	2.73	3.620 (7)	151.2
C6—H6B···Cl2	0.98	2.80	3.655 (7)	146.2

Symmetry code(s): (i) $-x+3/2, -y+1, z+1/2$; (ii) $-x+1, y+1/2, -z$; (iii) $-x+2, y+1/2, -z$;

(iv) $-x+3/2, y+1/2, z+1/2$.

Table S7. Selected bond lengths and angles for **2_100K**.

Bond lengths, Å			
Bi1—Cl2	2.602 (2)	Bi1—Cl1	2.846 (2)
Bi1—Cl3	2.560 (2)	Bi1—Cl1 ⁱⁱ	2.909 (2)
Bi1—Cl4	2.691 (2)	I1—I1 ⁱ	2.7167 (9)
Bi1—Cl4 ⁱ	2.691 (2)		
Bond angles, °			
Cl2—Bi1—Cl4	87.86 (4)	Cl3—Bi1—Cl1 ⁱⁱ	166.44 (8)
Cl2—Bi1—Cl4 ⁱ	87.86 (4)	Cl4—Bi1—Cl4 ⁱ	174.76 (8)
Cl2—Bi1—Cl1 ⁱⁱ	98.15 (8)	Cl4 ⁱ —Bi1—Cl1 ⁱⁱ	91.80 (4)
Cl2—Bi1—Cl1	179.79 (8)	Cl4—Bi1—Cl1	92.13 (4)
Cl3—Bi1—Cl2	95.42 (7)	Cl4—Bi1—Cl1 ⁱⁱ	91.80 (4)
Cl3—Bi1—Cl4	88.69 (4)	Cl4 ⁱ —Bi1—Cl1	92.13 (4)
Cl3—Bi1—Cl4 ⁱ	88.69 (4)	Cl1—Bi1—Cl1 ⁱⁱ	82.07 (2)
Cl3—Bi1—Cl1	84.37 (8)	Bi1—Cl1—Bi1 ⁱⁱⁱ	156.81 (12)

Symmetry code(s): (i) $x, -y+1/2, z$; (ii) $x+1/2, y, -z+3/2$; (iii) $x-1/2, y, -z+3/2$.

Table S8. Selected hydrogen bond parameters for **2_100K**.

D—H···A	D—H (Å)	H···A (Å)	D···A (Å)	D—H···A (°)
C2—H2···Cl4 ⁱ	0.95	2.94	3.804 (9)	151.8
C5—H5···Cl4 ⁱⁱ	0.95	2.61	3.532 (8)	163.4
N1—H1A···Cl1 ⁱⁱⁱ	0.88	2.68	3.356 (10)	134.0
C6—H6A···Cl3	0.99	2.68	3.579 (14)	150.6
C6—H6B···Cl2	0.99	2.77	3.632 (15)	146.2
C9—H9···Cl3	0.95	3.05	3.894 (10)	149.2
C10—H10···Cl4	0.95	3.21	3.970 (10)	138.5
N2—H2A···Cl2 ^{iv}	0.88	2.45	3.144 (10)	136.3
N2—H2A···Cl3 ^v	0.88	2.72	3.368 (11)	131.5
C11—H11···Cl4 ^{vi}	0.95	3.04	3.693 (11)	127.4
C11—H11···Cl1 ^v	0.95	2.82	3.439 (11)	124.0
C12—H12···Cl4 ^{vi}	0.95	3.09	3.720 (11)	124.9

Symmetry code(s): (i) $x, -y+1/2, z$; (ii) $-x+1/2, y+1/2, z-1/2$; (iii) $-x, y+1/2, -z+1$; (iv) $-x+1, y-1/2, -z+1$; (v) $-x, y-1/2, -z+1$; (vi) $-x+1/2, -y, z-1/2$.

Table S9. Selected bond lengths and angles for **3**.

Bond length, Å			
Sb1—Cl1	2.6211 (7)	Sb1—Cl3	2.3970 (8)
Sb1—Cl1 ⁱ	2.6211 (7)	Sb1—Cl4	2.4770 (9)
Sb1—Cl2	2.8146 (9)	I1—I1 ⁱⁱ	2.7156 (4)
Bond angle, (°)			
Cl1 ⁱⁱ —Sb1—Cl1	170.23 (3)	Cl3—Sb1—Cl2	82.31 (3)
Cl1 ⁱⁱ —Sb1—Cl2	87.058 (16)	Cl3—Sb1—Cl4	88.85 (3)
Cl1—Sb1—Cl2	87.058 (16)	Cl4—Sb1—Cl1 ⁱⁱ	92.308 (16)
Cl3—Sb1—Cl1	85.742 (15)	Cl4—Sb1—Cl1	92.308 (16)
Cl3—Sb1—Cl1 ⁱⁱ	85.742 (16)	Cl4—Sb1—Cl2	171.16 (3)

Symmetry code(s): (i) $x, -y+1/2, z$; (ii) $x, -y+3/2, z$.**Table S10.** Selected hydrogen bond parameters for **3**.

D—H···A	D—H (Å)	H···A (Å)	D···A (Å)	D—H···A (°)
N1—H1···Cl2 ⁱ	0.87	2.31	3.136 (2)	158.1
N1—H1···Cl3 ⁱ	0.87	3.09	3.645 (2)	123.9
C2—H2···Cl1 ⁱⁱ	0.94	3.01	3.724 (3)	134.3
C2—H2···Cl3 ⁱⁱⁱ	0.94	3.18	3.809 (3)	126.2
C5—H5···Cl3 ⁱ	0.94	2.83	3.533 (3)	132.7
C6—H6B···Cl4 ⁱⁱⁱ	0.98	3.19	3.834 (3)	125.1
C7—H7A···Cl2 ^{iv}	0.98	2.75	3.645 (3)	152.5
C7—H7B···Cl3 ⁱⁱⁱ	0.98	2.86	3.834 (3)	170.8

Symmetry code(s): (i) $x-1/2, -y+3/2, -z+1/2$; (ii) $-x+1, -y+1, -z$; (iii) $-x+1, y-1/2, -z$; (iv) $-x+1, y-1/2, -z+1$.**Table S11.** Selected bond lengths and angles for **3_300K**.

Bond length, Å			
Sb1—Cl3	2.3955 (13)	Sb1—Cl1	2.6256 (13)
Sb1—Cl2	2.8217 (17)	Sb1—Cl1 ⁱ	2.6256 (13)
Sb1—Cl4	2.4734 (16)	I1—I1 ⁱⁱ	2.7155 (7)
Bond angle, (°)			
Cl1—Sb1—Cl1 ⁱ	170.83 (6)	Cl3—Sb1—Cl2	82.48 (5)
Cl1 ⁱ —Sb1—Cl2	87.19 (3)	Cl3—Sb1—Cl4	88.93 (5)
Cl1—Sb1—Cl2	87.19 (3)	Cl4—Sb1—Cl1	92.24 (3)
Cl3—Sb1—Cl1 ⁱ	86.05 (3)	Cl4—Sb1—Cl1 ⁱ	92.24 (3)
Cl3—Sb1—Cl1	86.05 (3)	Cl4—Sb1—Cl2	171.41 (5)

Symmetry code(s): (i) $x, -y+3/2, z$.**Table S12.** Selected hydrogen bond parameters for **3_300K**.

D—H···A	D—H (Å)	H···A (Å)	D···A (Å)	D—H···A (°)
N1—H1···Cl2 ⁱ	0.86	2.33	3.151 (5)	158.5
C1—H1A···Cl3 ⁱ	0.93	2.85	3.554 (6)	133.4

Symmetry code(s): (i) $-x+3/2, -y+1, z-1/2$.

Table S13. Selected bond lengths and angles for **4**.

Bond length, Å			
Bi1—Cl3	2.6585 (11)	Bi1—Cl2	2.5550 (12)
Bi1—Cl4 ⁱ	2.9046 (12)	Bi1—Cl1	2.7145 (12)
Bi1—Cl4	2.7979 (12)	I1—I2	2.7109 (5)
Bi1—Cl5	2.6631 (11)		
Bond angle, (°)			
Cl3—Bi1—Cl4 ⁱ	83.40 (3)	Cl2—Bi1—Cl3	92.99 (4)
Cl3—Bi1—Cl4	177.18 (3)	Cl2—Bi1—Cl4	88.47 (4)
Cl3—Bi1—Cl5	87.14 (3)	Cl2—Bi1—Cl4 ⁱ	176.39 (4)
Cl3—Bi1—Cl1	86.34 (4)	Cl2—Bi1—Cl5	93.18 (4)
Cl4—Bi1—Cl4 ⁱ	95.140 (12)	Cl2—Bi1—Cl1	93.89 (4)
Cl5—Bi1—Cl4	95.20 (4)	Cl1—Bi1—Cl4	91.15 (4)
Cl5—Bi1—Cl4 ⁱ	86.57 (4)	Cl1—Bi1—Cl4 ⁱ	85.99 (4)
Cl5—Bi1—Cl1	170.62 (4)	Bi1—Cl4—Bi1 ⁱⁱ	153.14 (5)

Symmetry code(s): (i) $x, -y+3/2, z-1/2$; (ii) $x, -y+3/2, z+1/2$.**Table S14.** Selected hydrogen bond parameters for **4**.

D—H···A	D—H (Å)	H···A (Å)	D···A (Å)	D—H···A (°)
N1—H1···Cl3 ⁱ	0.88	2.52	3.293 (4)	146.4
N2—H2···Cl3 ⁱⁱ	0.88	2.37	3.215 (4)	159.6
C10—H10···Cl4 ⁱⁱⁱ	0.95	2.72	3.505 (5)	140.5

Symmetry code(s): (i) $-x+1, -y+1, -z+1$; (ii) $-x+2, -y+1, -z+1$; (iii) $-x+2, y-1/2, -z+3/2$.

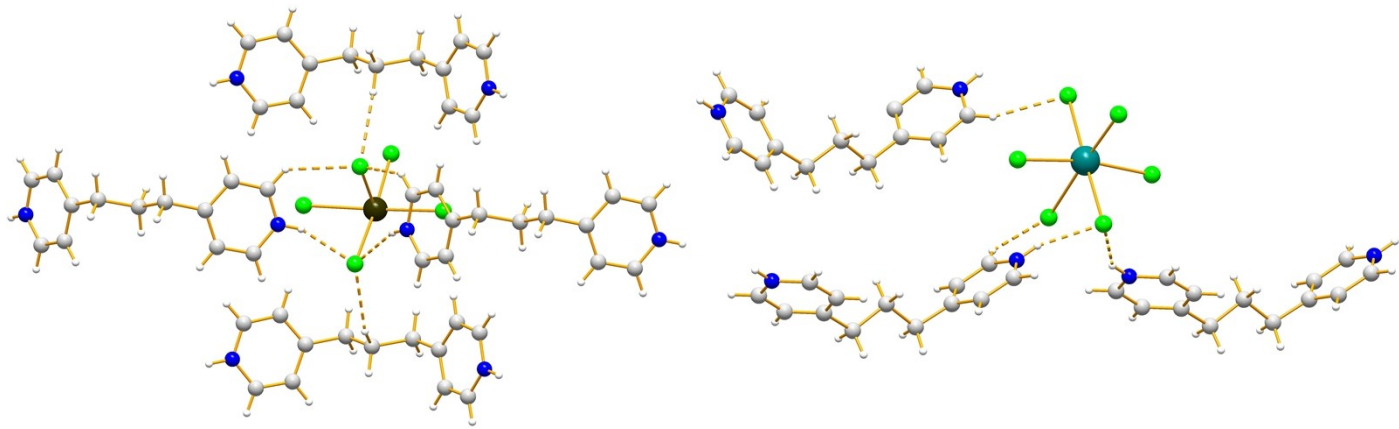


Figure S1. Hydrogen bonds (dashed) in crystal structures of **3** (*left*) and **4** (*right*).

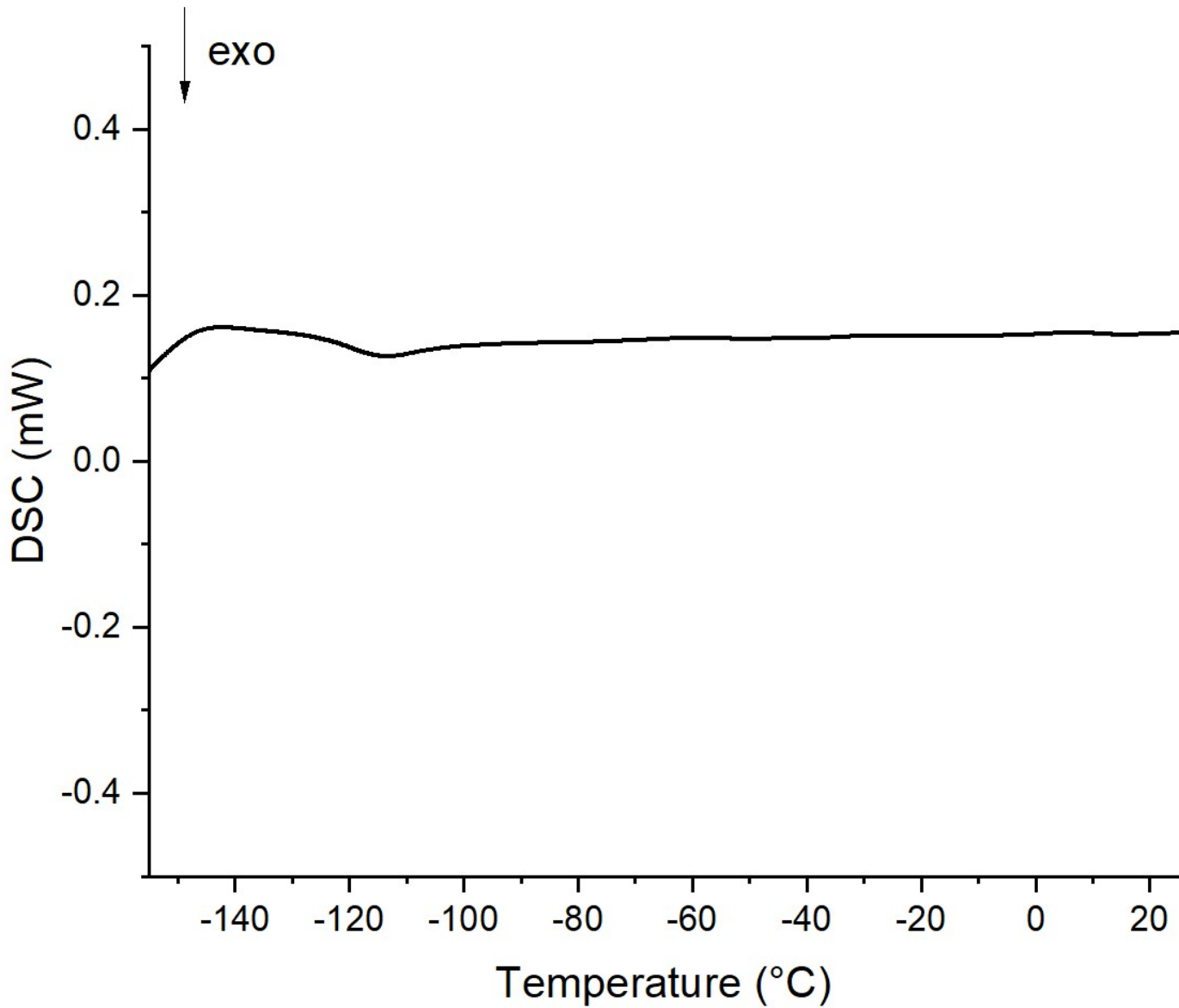


Figure S2. DSC curve for $(\text{H}_2\text{bpe})\{\text{[SbCl}_5](\text{I}_2)\}$ (**1**).

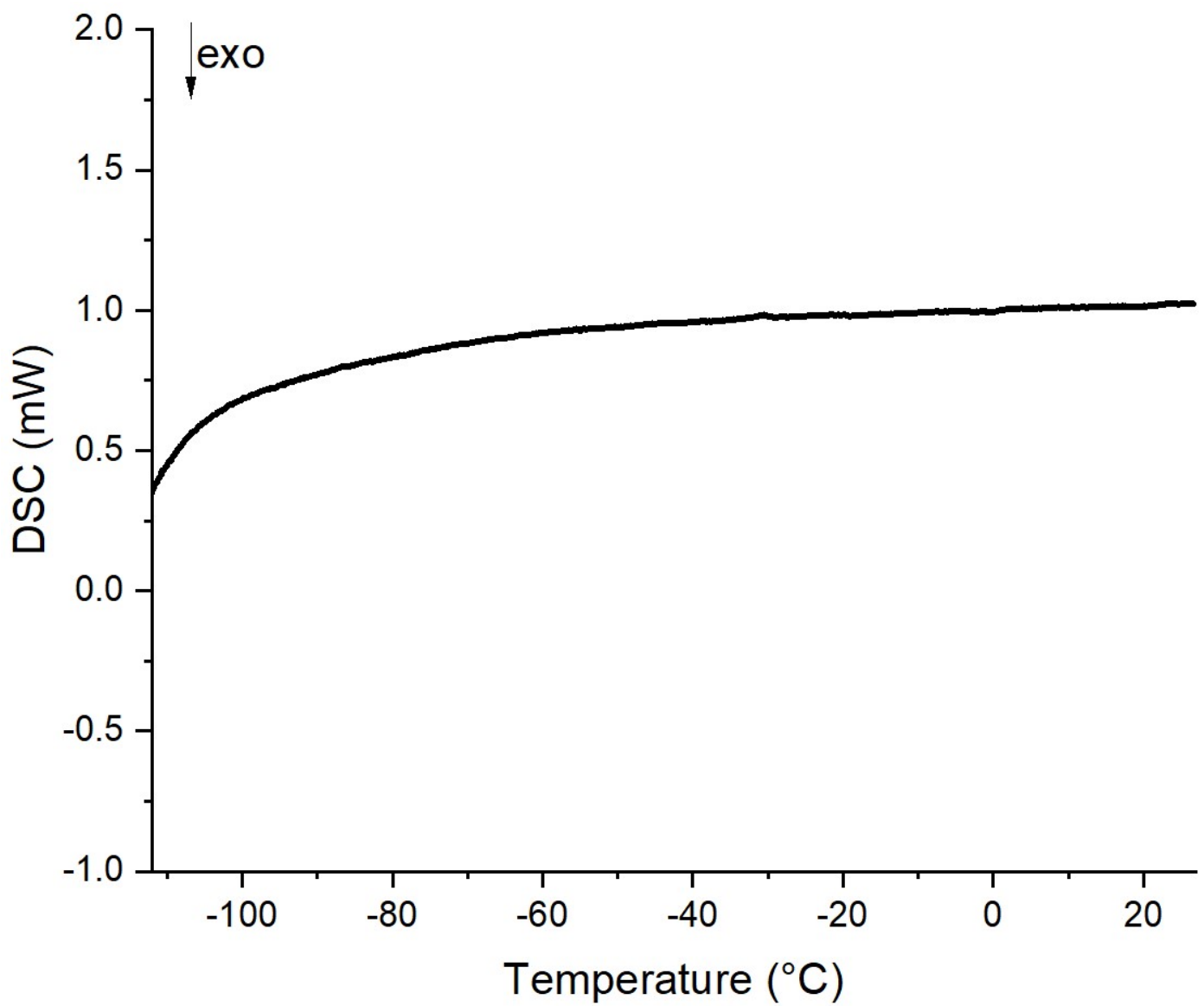


Figure S3. DSC curve for $(\text{H}_2\text{bpp})\{\text{[SbCl}_5\text{]}\text{(I}_2\text{)}\}$ (**3**).

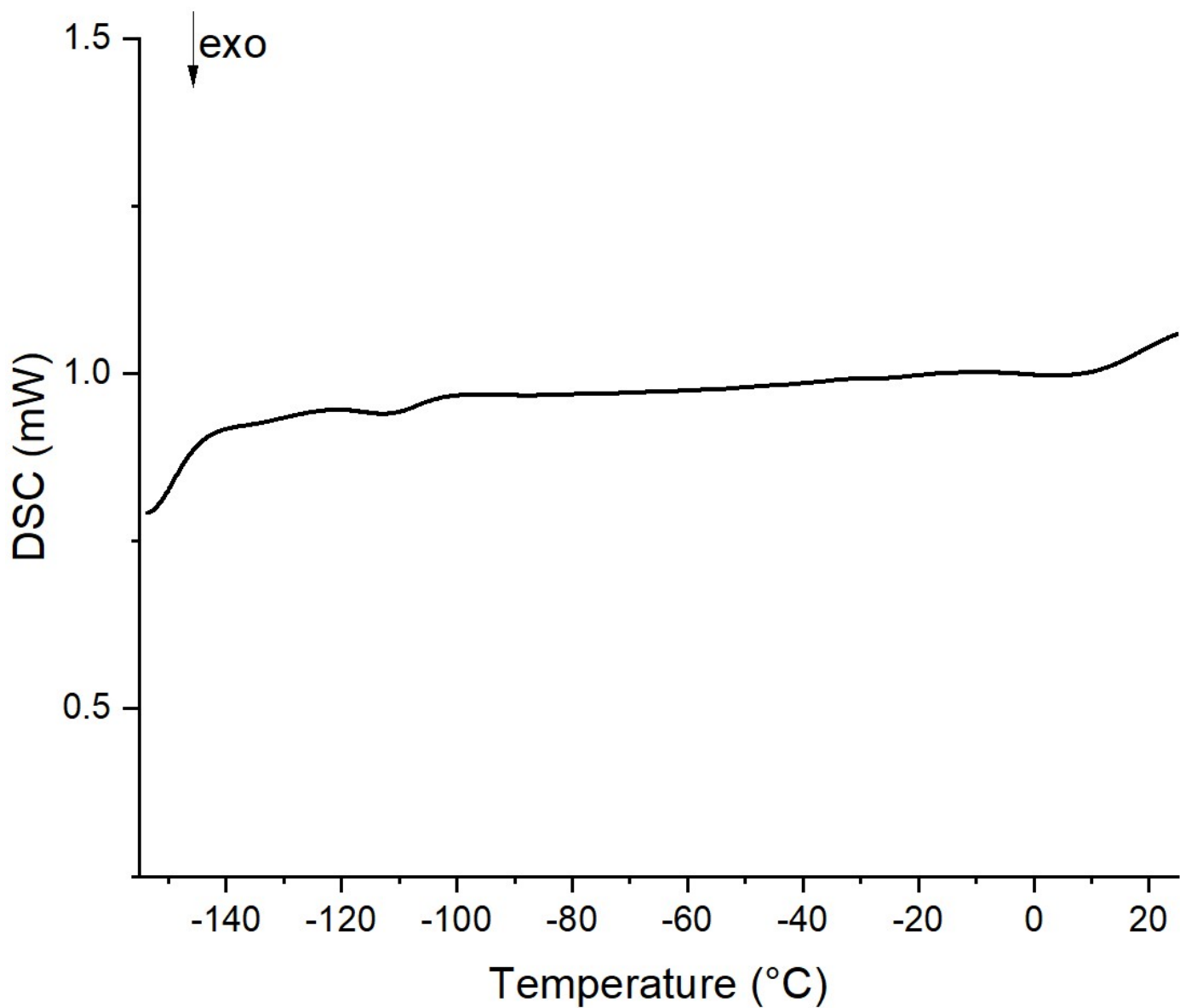


Figure S4. DSC curve for $(\text{H}_2\text{bpp})\{\text{[BiCl}_5\text{]}\text{(I}_2\text{)}\}$ (**4**).

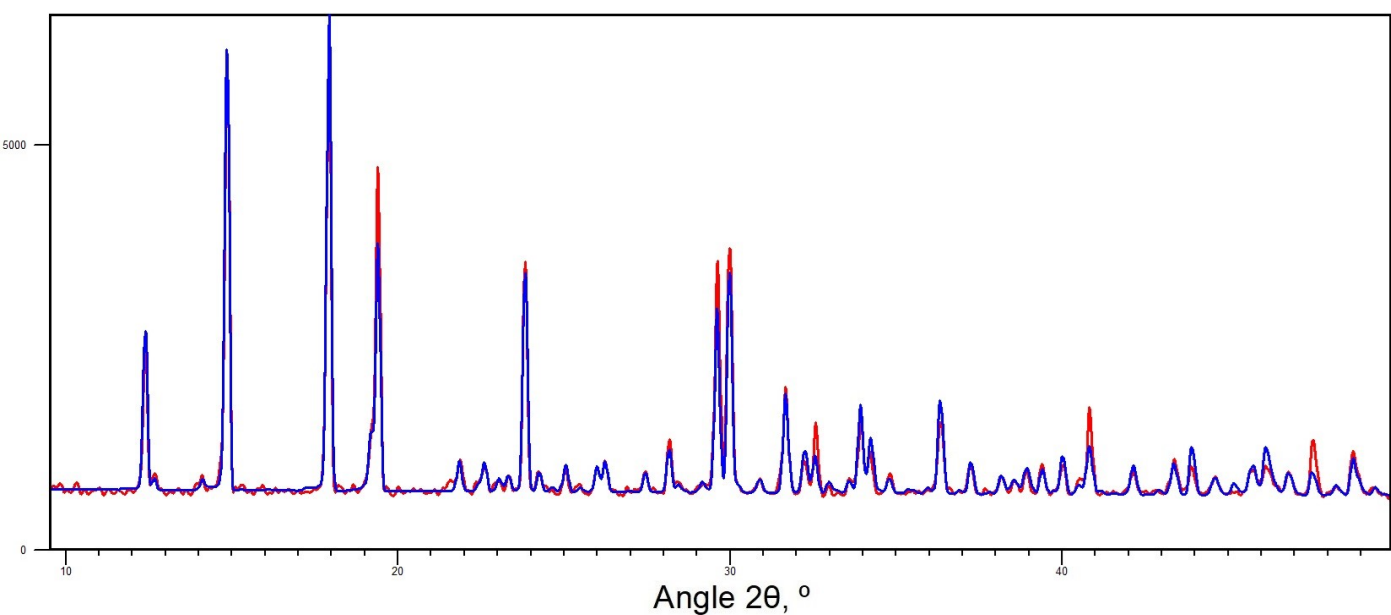


Figure S5. Experimental (red) and calculated from SCXRD data (blue) powder patterns comparison for **1**.

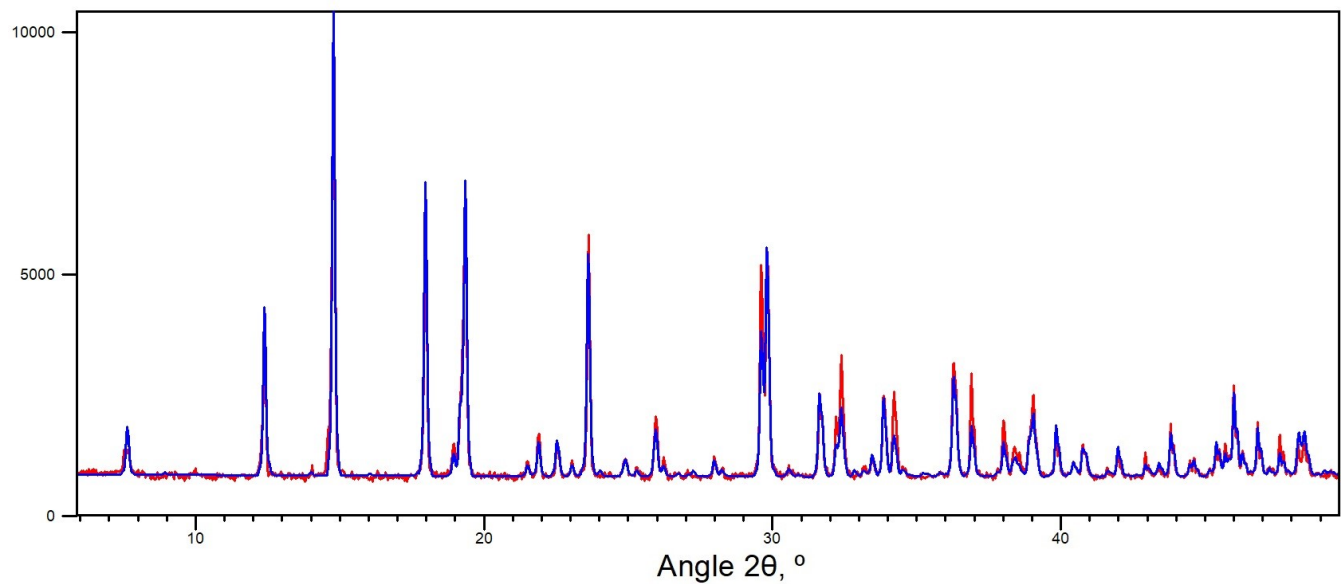


Figure S6. Experimental (red) and calculated from SCXRD data (blue) powder patterns comparison for **2**.

Fig

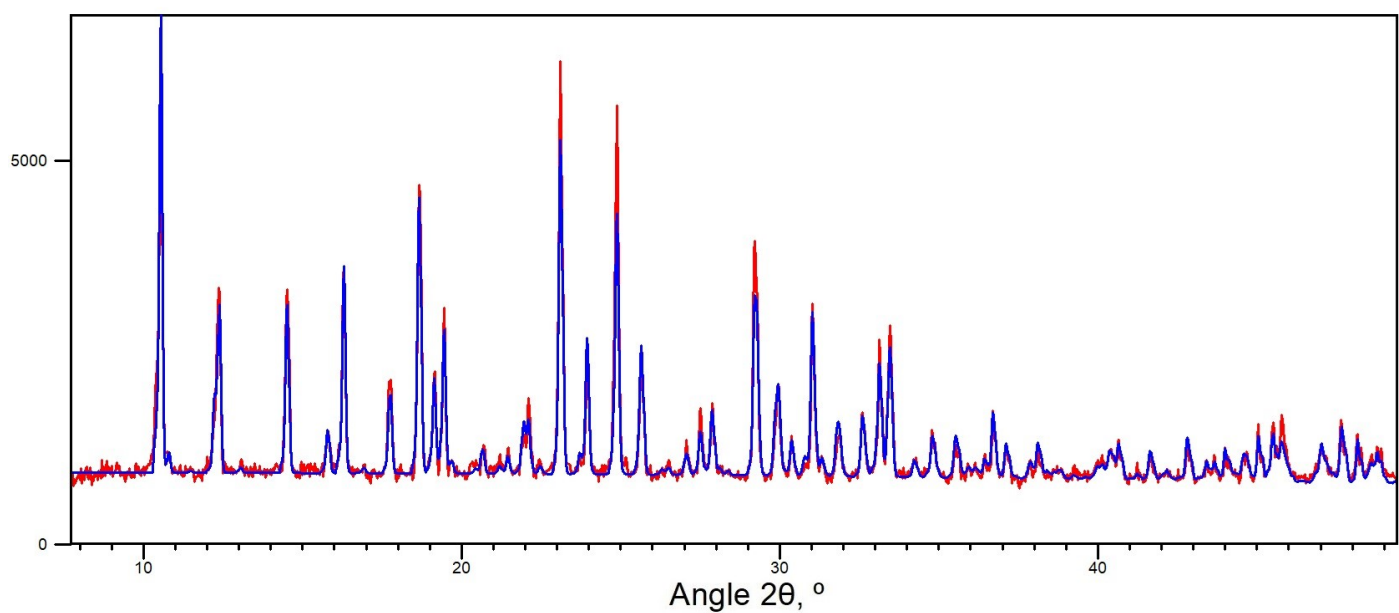


Figure S7. Experimental (red) and calculated from SCXRD data (blue) powder patterns comparison for **3**.

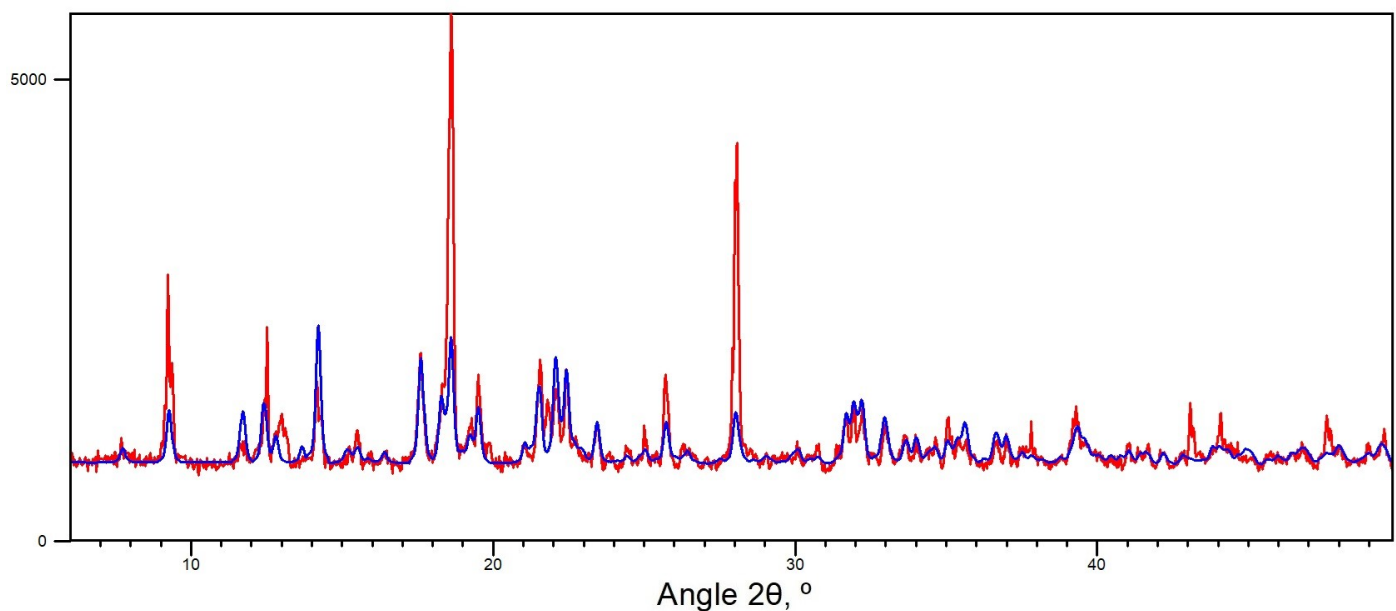


Figure S8. Experimental (red) and calculated from SCXRD data (blue) powder patterns comparison for **4**.

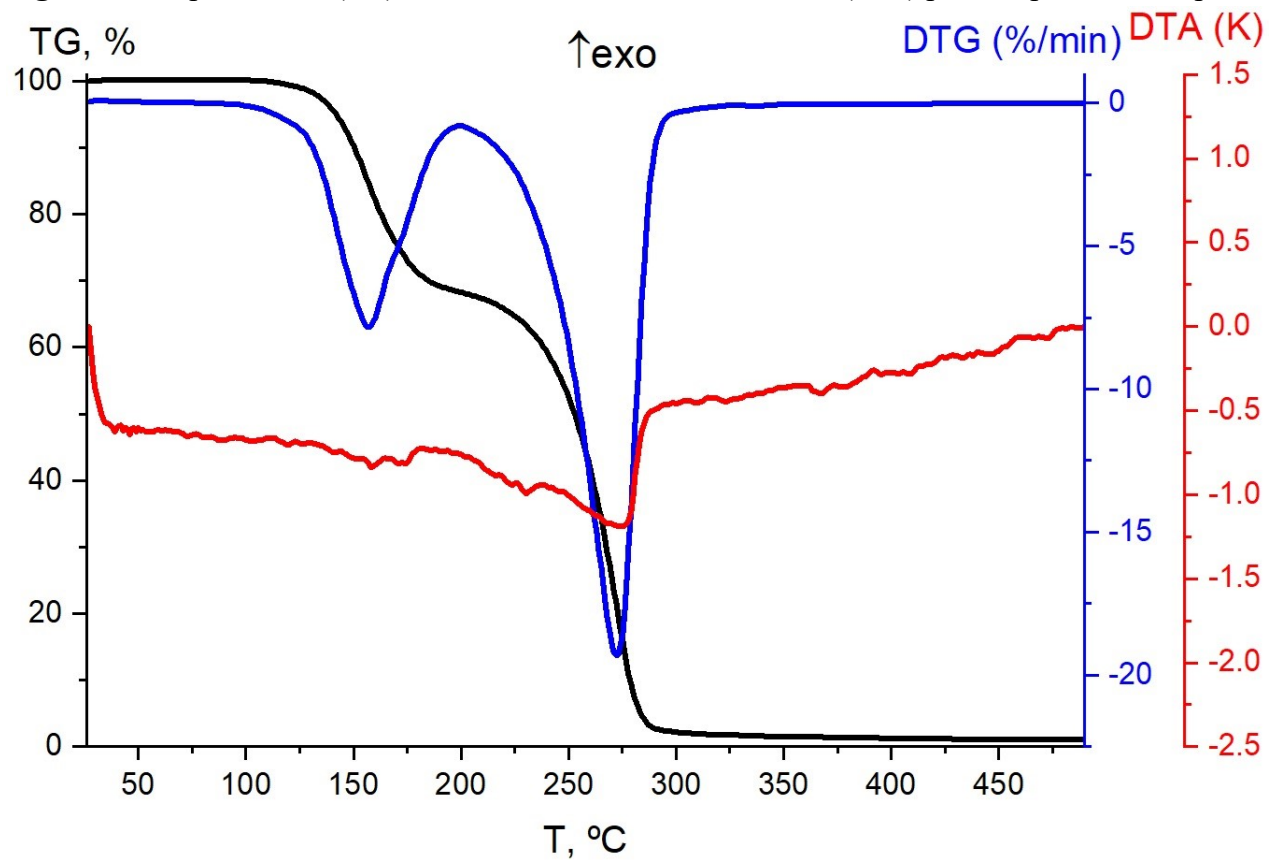


Figure S9. TG, DTG and DTA curves for **3**.

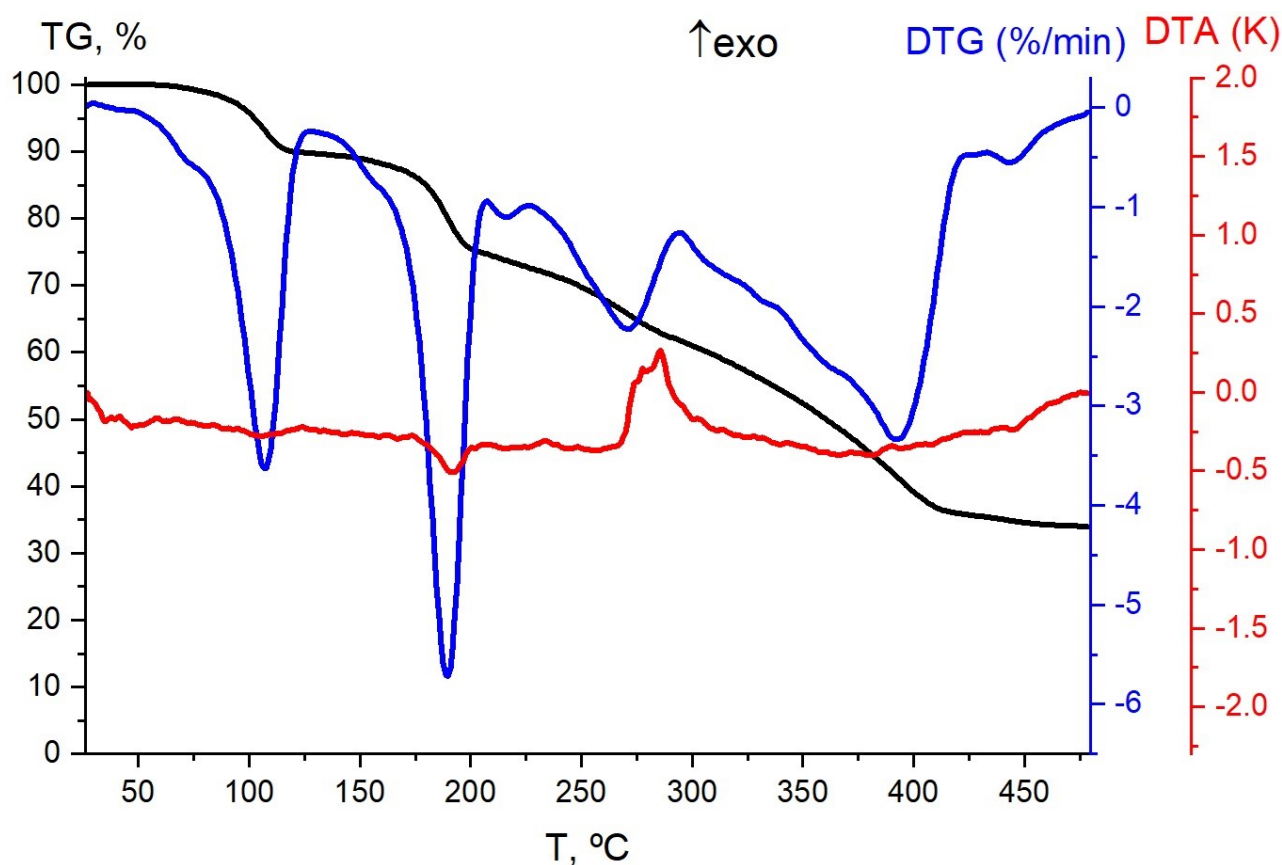


Figure S10. TG, DTG and DTA curves for 4.

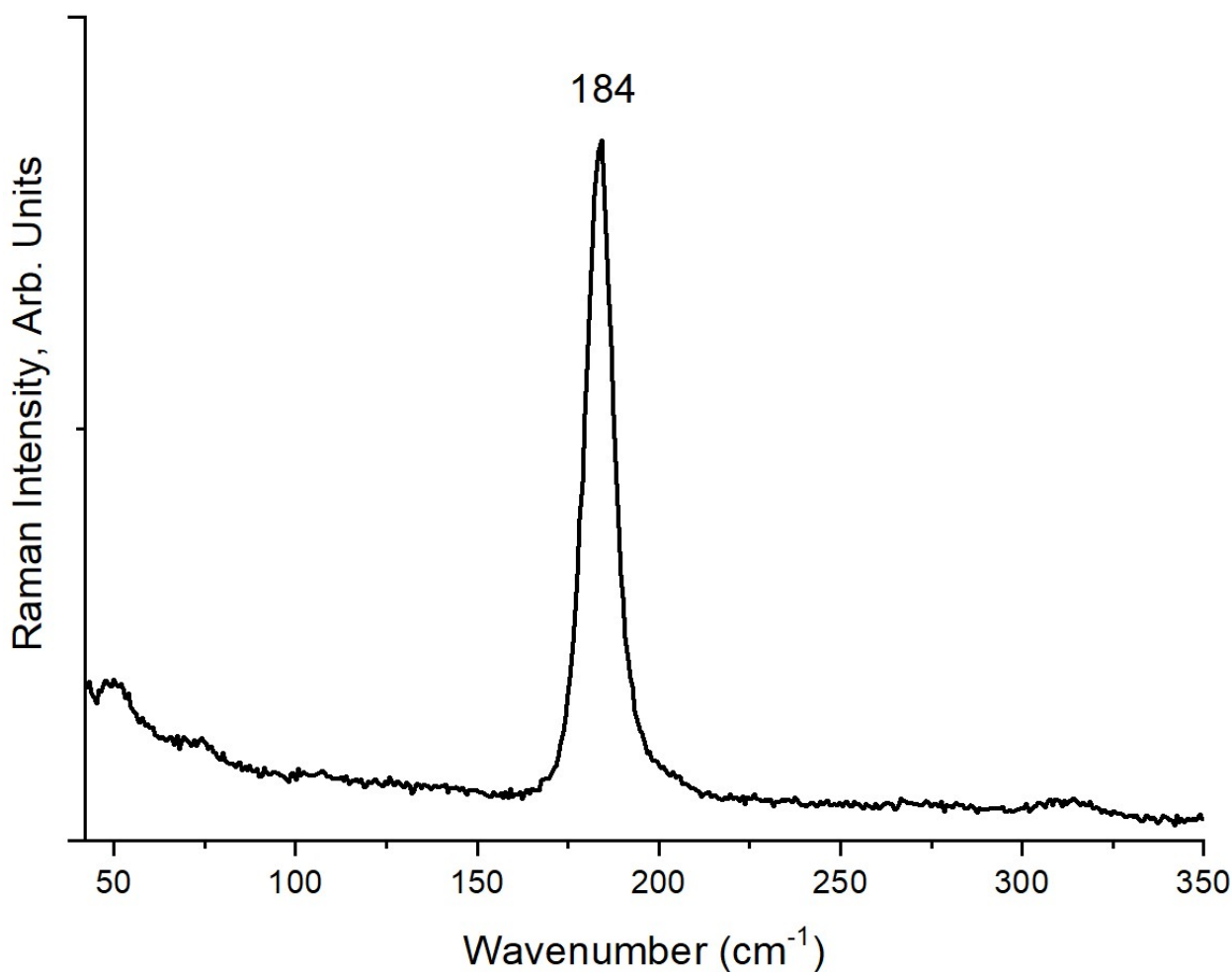


Figure S11. Raman spectrum of 1.

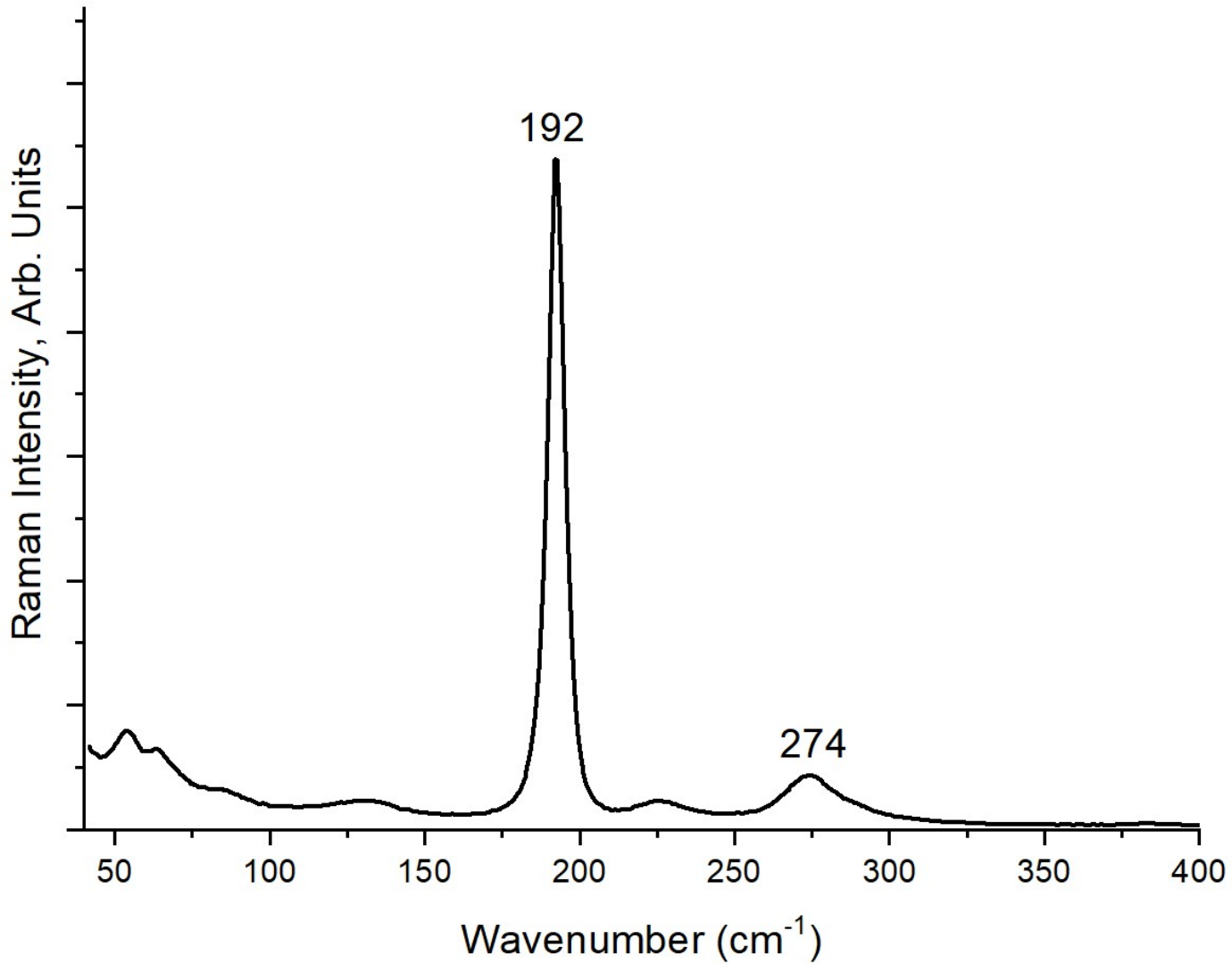


Figure S12. Raman spectrum of **2**.

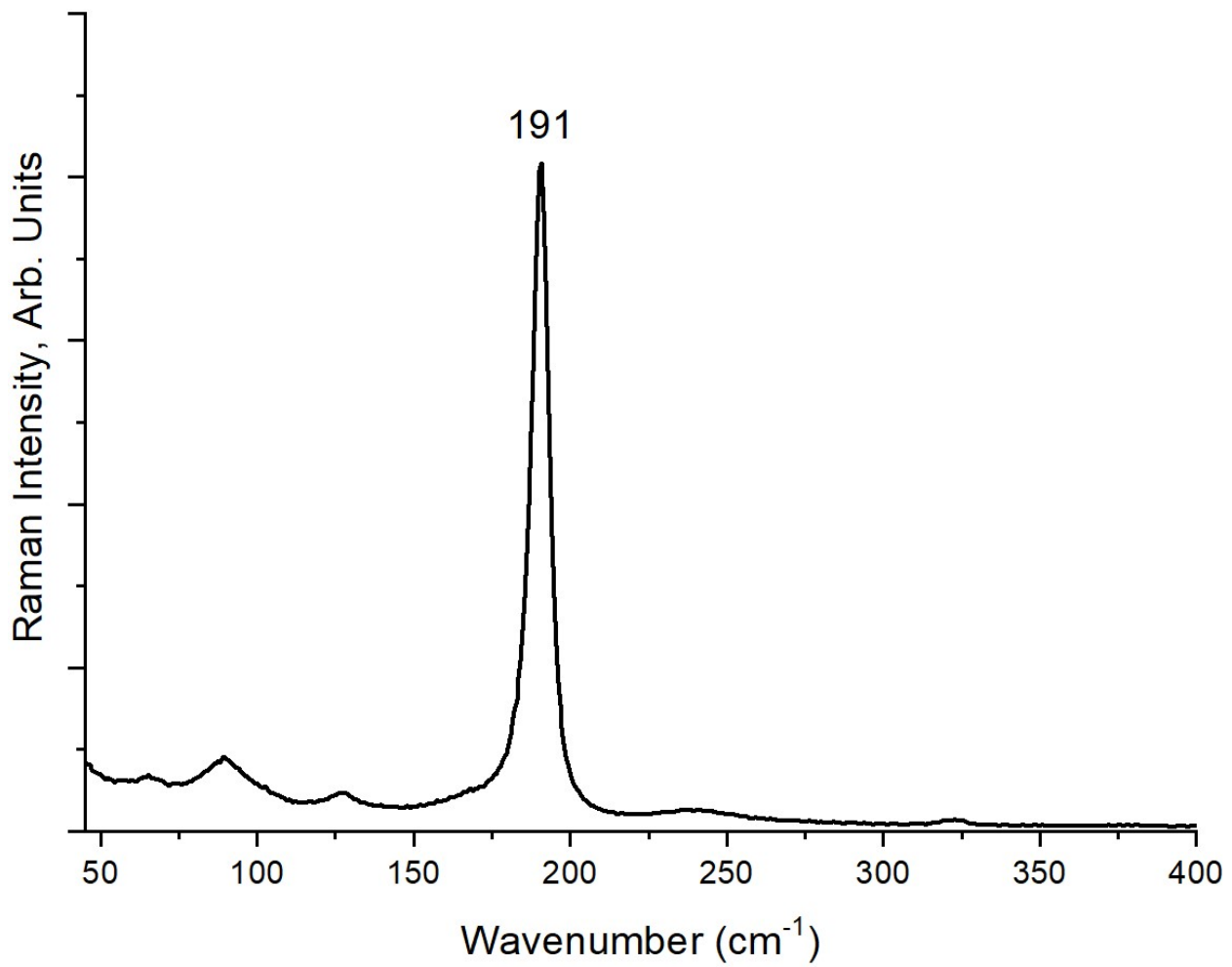


Figure S13. Raman spectrum of **3**.

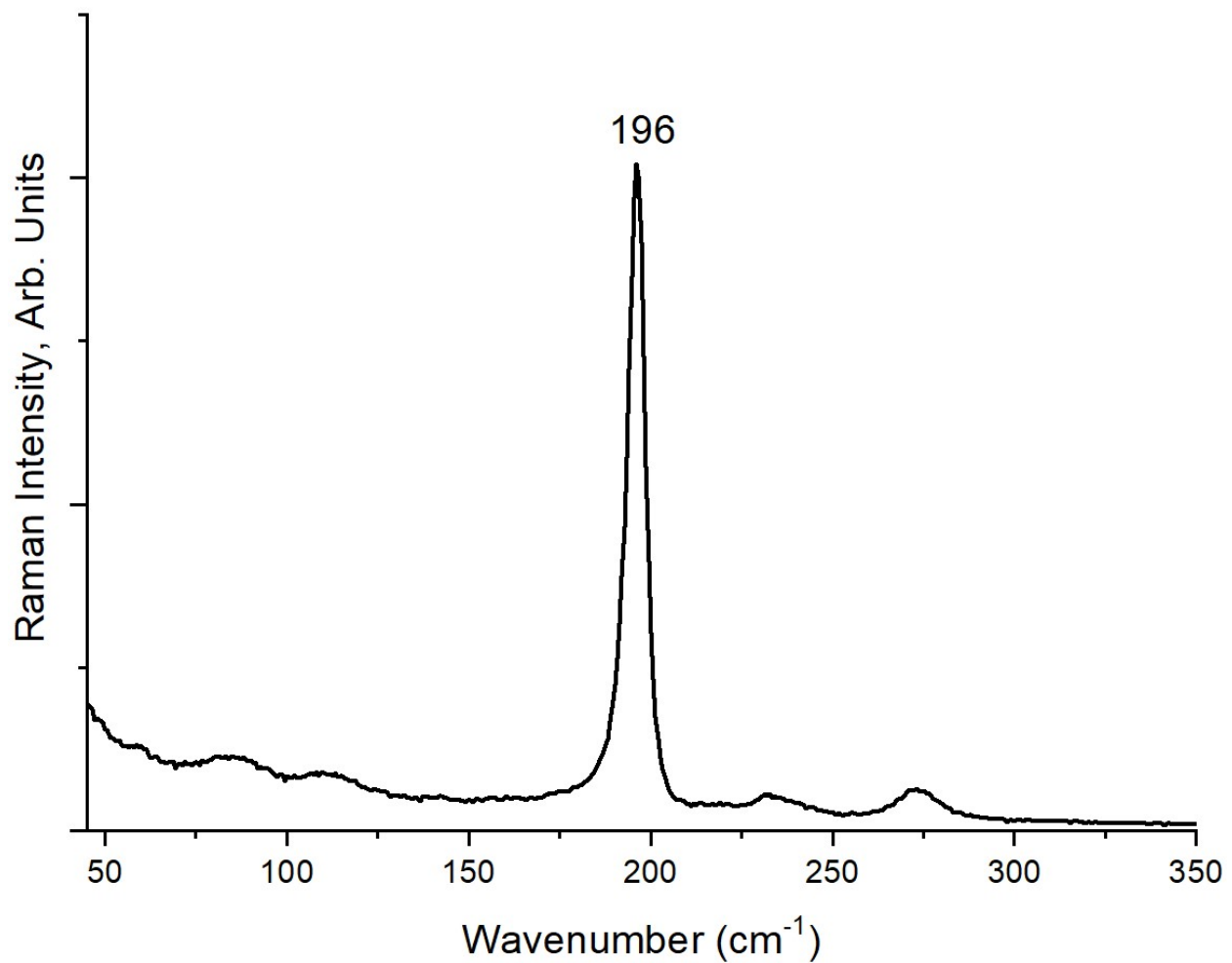


Figure S14. Raman spectrum of **4**.

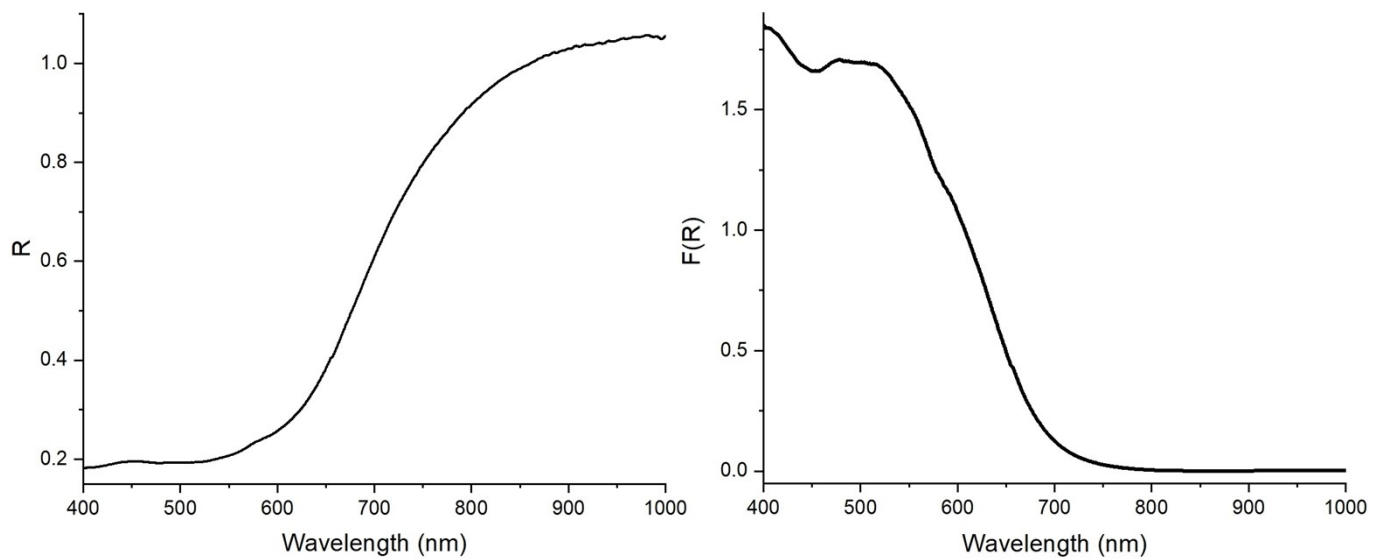


Figure S15. Diffuse reflectance spectrum (*left*) and Cubelka-Munk function (*right*) for **1**.

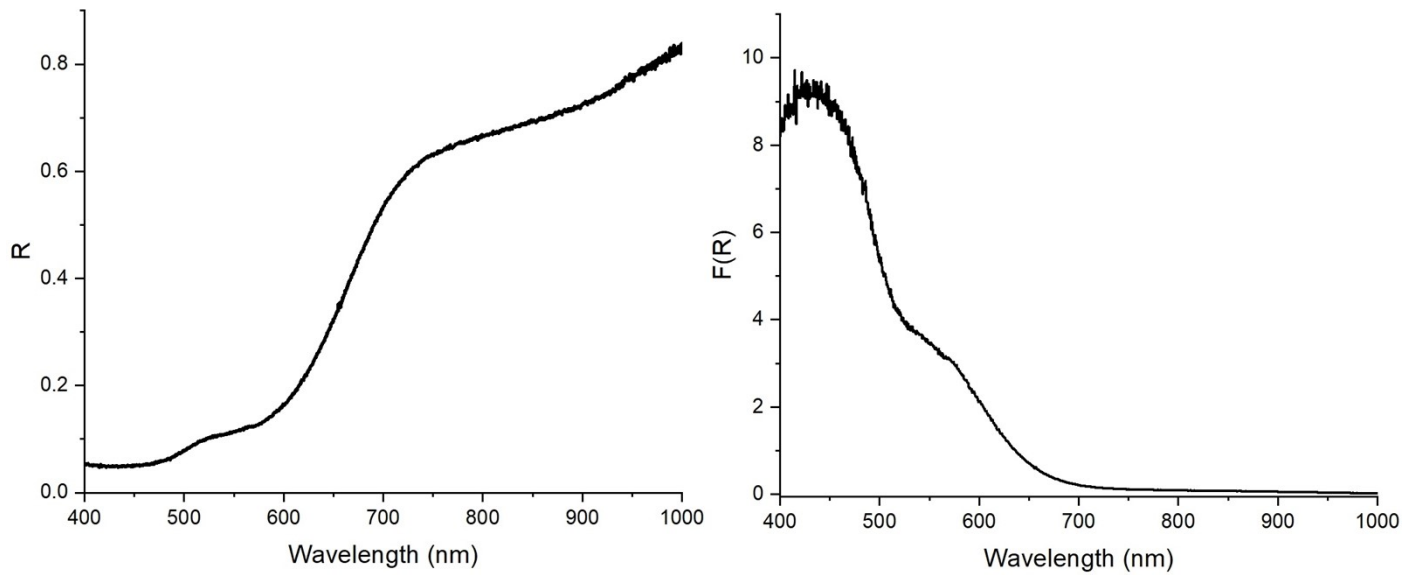


Figure S16. Diffuse reflectance spectrum (*left*) and Cubelka-Munk function (*right*) for **2**.

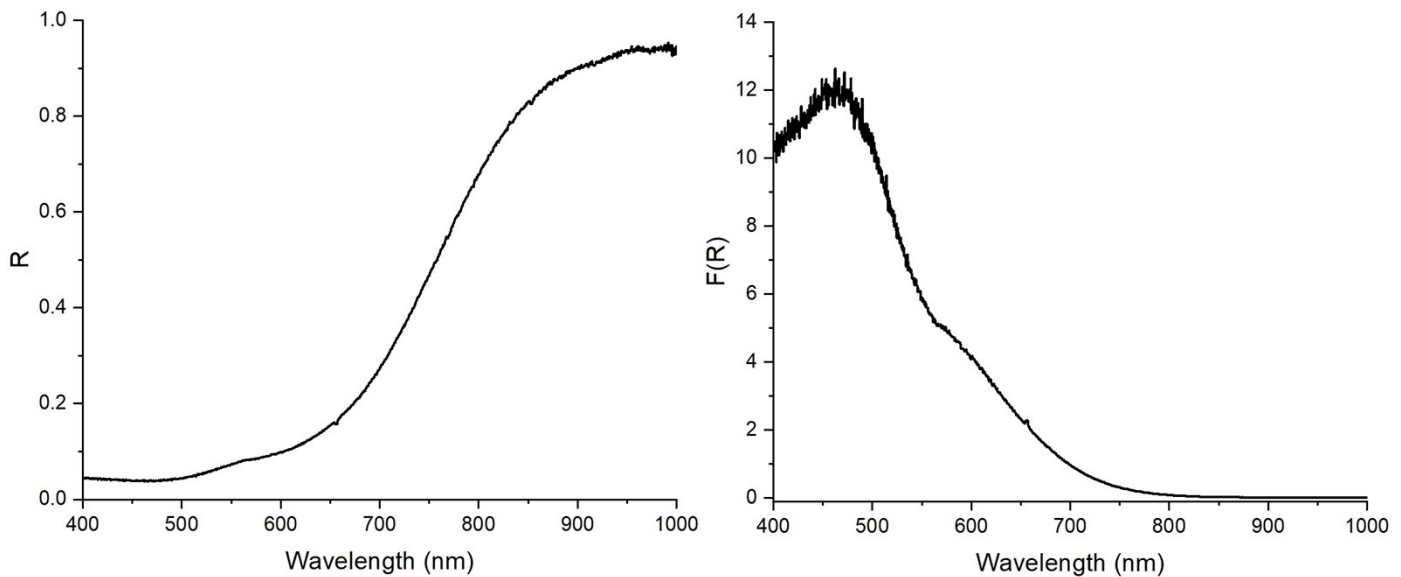


Figure S17. Diffuse reflectance spectrum (*left*) and Cubelka-Munk function (*right*) for **3**.

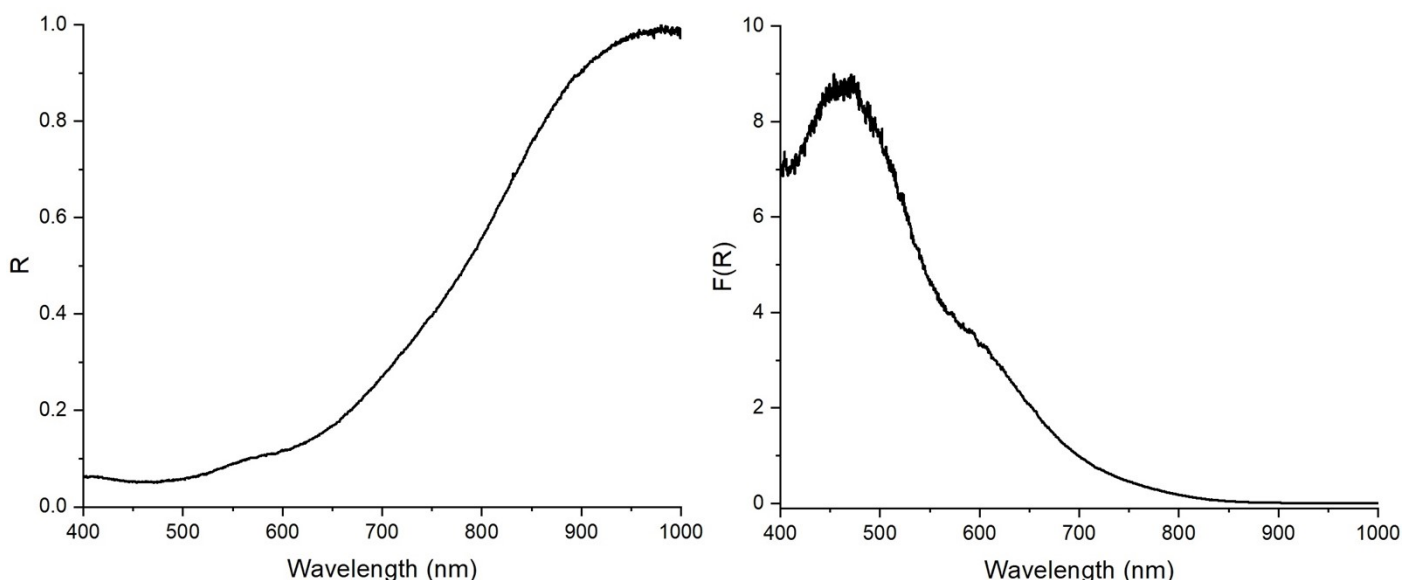


Figure S18. Diffuse reflectance spectrum (*left*) and Cubelka-Munk function (*right*) for **4**.

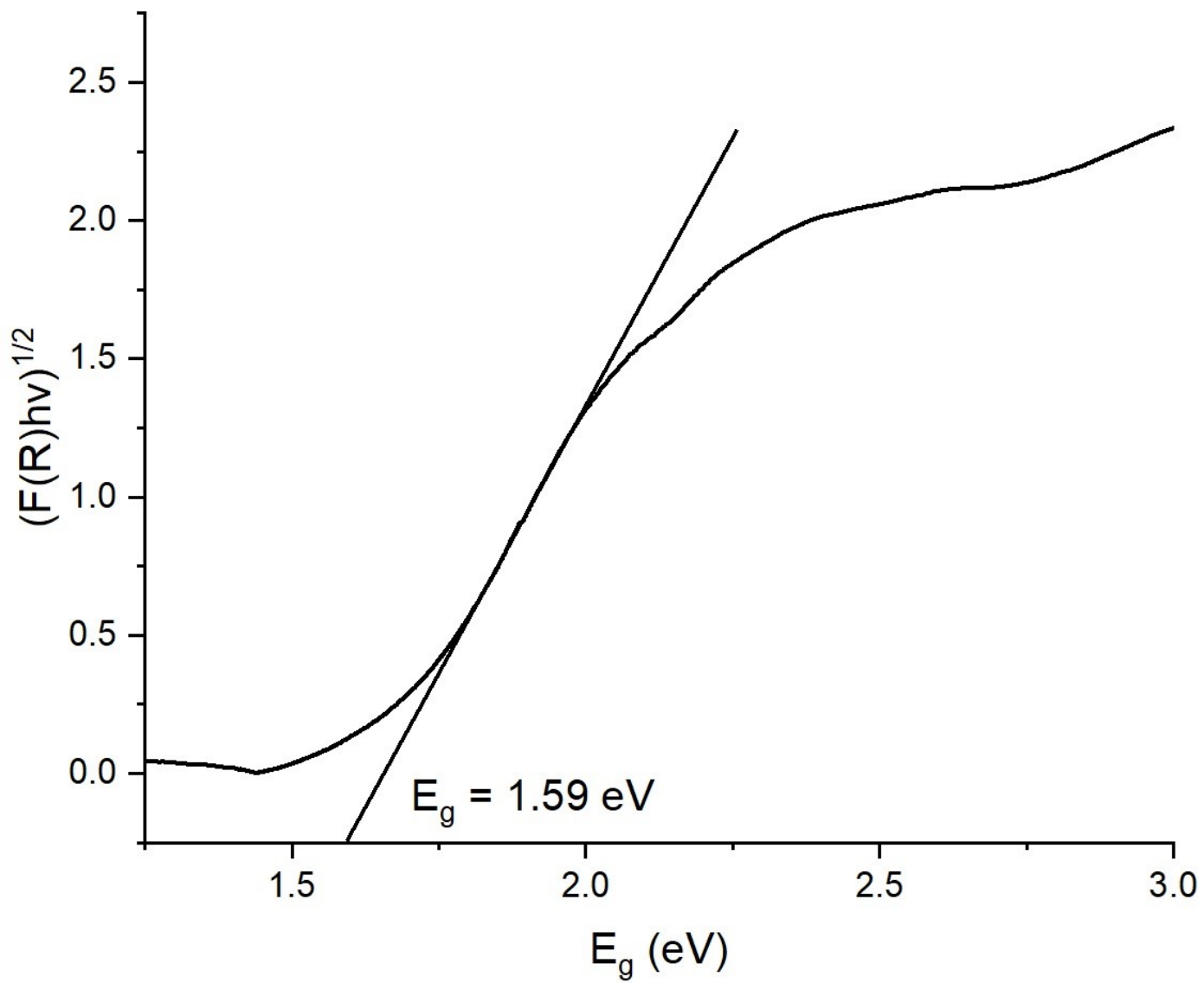


Figure S19. Band gap determination for **1**.

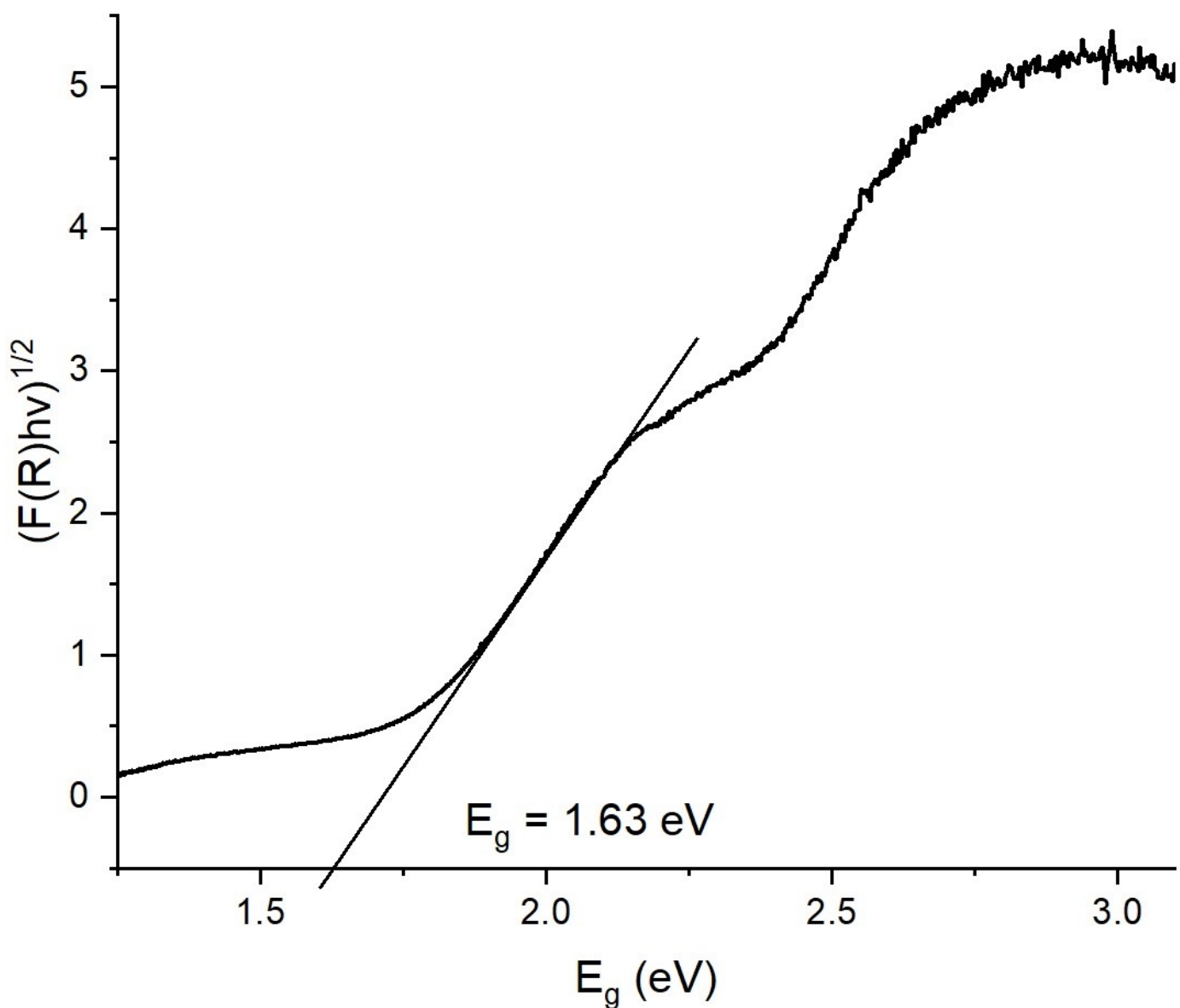


Figure S20. Band gap determination for 2.

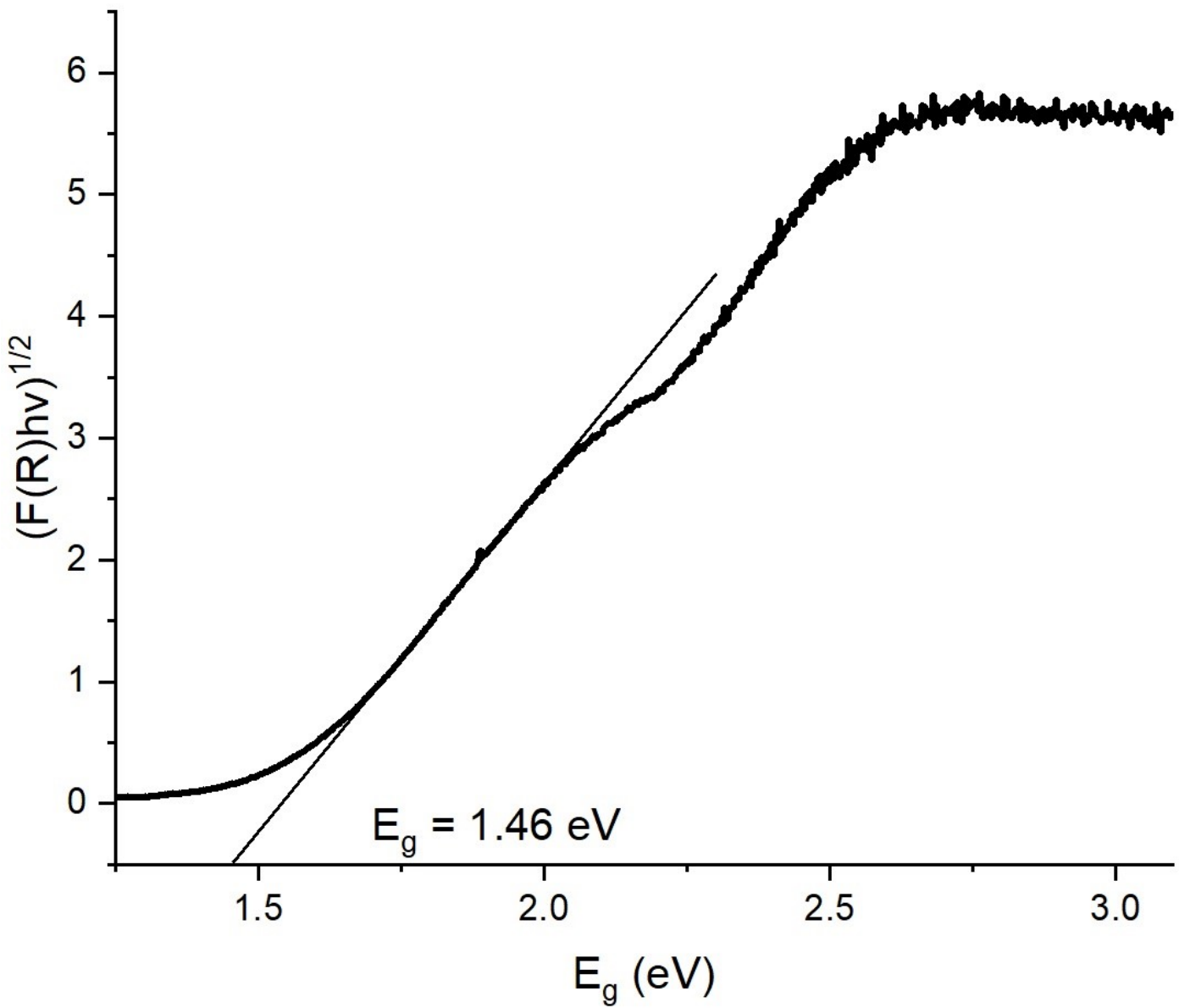


Figure S21. Band gap determination for **3**.

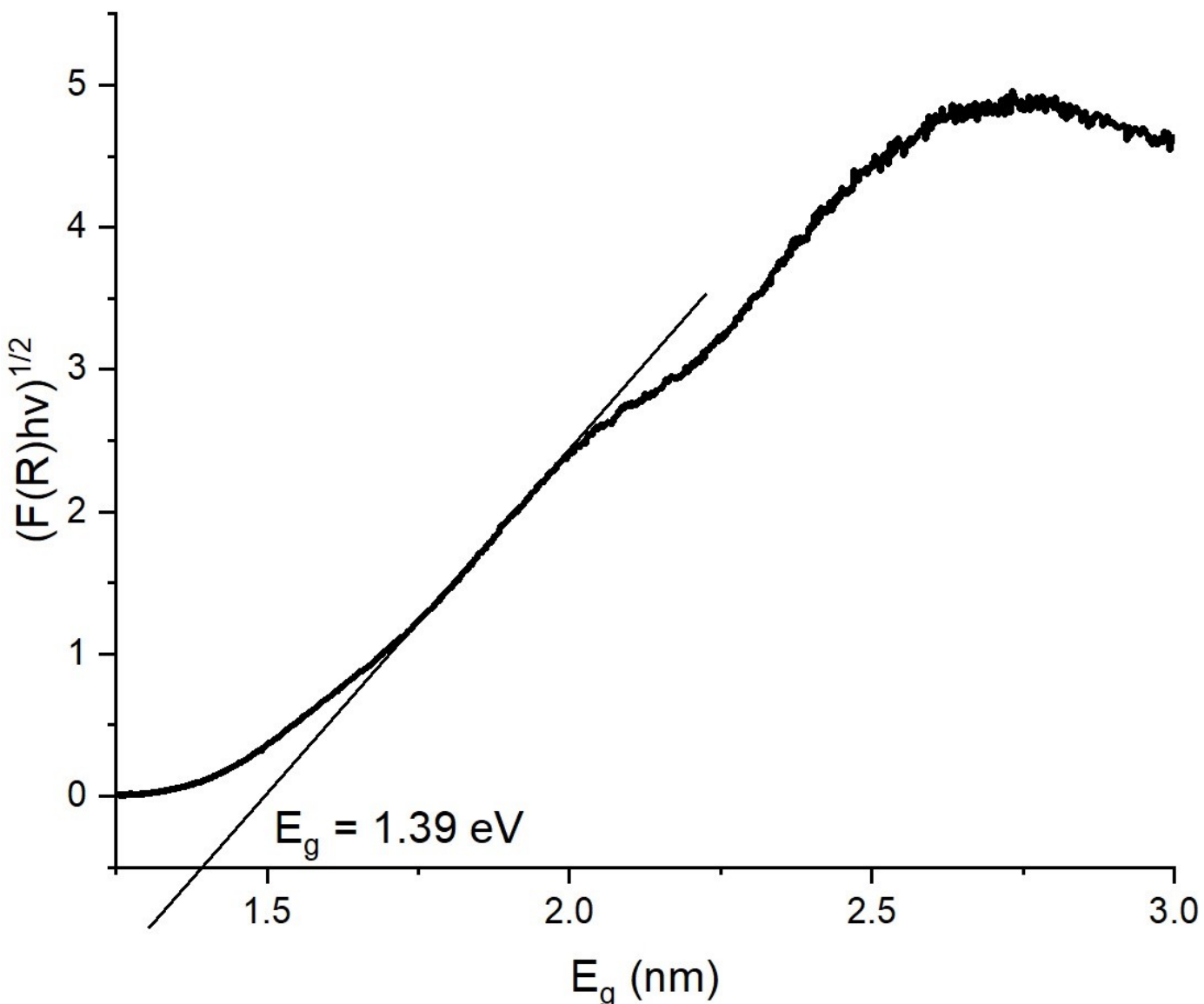


Figure S22. Band gap determination for **4**.

Computational details

The single point calculations based on the experimental X-ray geometries of **2**, **3**, and **4** have been carried out at the DFT level of theory using the dispersion-corrected hybrid functional ω B97XD [Phys. Chem. Chem. Phys. 2008, 10, 6615.] with the help of Gaussian-09 [M. J. Frisch et al., Gaussian 09, Revision C.01, Gaussian, Inc., Wallingford, CT, 2010.] program package. The Douglas–Kroll–Hess 2nd order scalar relativistic calculations requested relativistic core Hamiltonian were carried out using the DZP-DKH basis sets [Mol. Phys. 2010, 108, 1965. || J. Chem. Phys. 2009, 130, 064108. || Chem. Phys. Lett. 2013, 582, 158. || J. Mol. Struct. - Theochem 2010, 961, 107.] for all atoms. The topological analysis of the electron density distribution (QTAIM), electron localization function (ELF), reduced density gradient (RDG) and interaction region indicator (IRI) analyses [Chemistry–Methods 2021, 1, 231.] have been performed by using the Multiwfn program (version 3.7) [J. Comput. Chem. 2012, 33, 580.]. The VMD program [J. Molec. Graphics 1996, 14, 33.] was used for visualization. The Cartesian atomic coordinates for model supramolecular associates presented in **Table S6**.

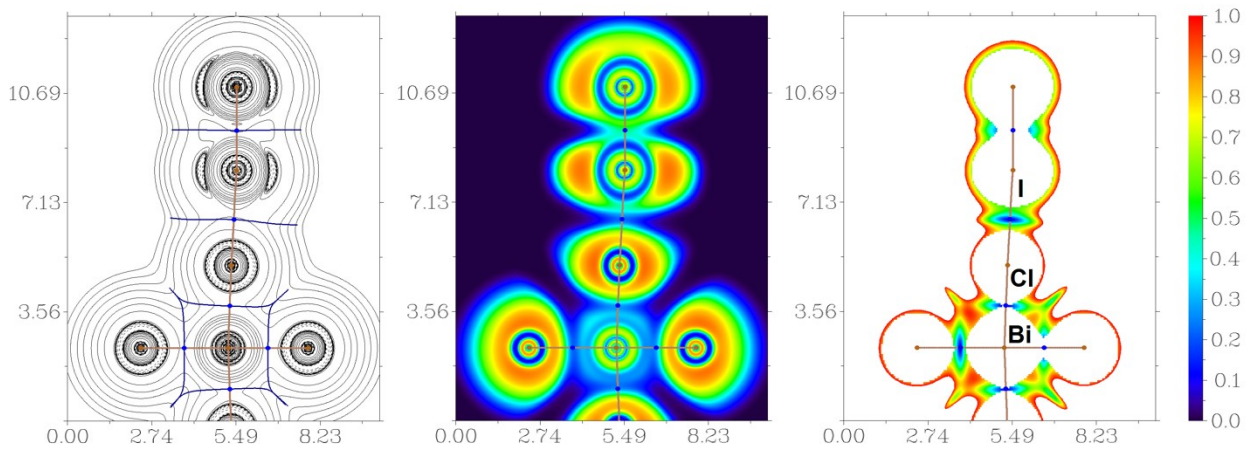


Figure S23. Contour line diagram of the Laplacian of electron density distribution $\nabla^2\rho(\mathbf{r})$, bond paths, and selected zero-flux surfaces (left panel), visualization of electron localization function (ELF, center panel) and reduced density gradient (RDG, right panel) analyses for intermolecular interactions $\text{I}\cdots\text{Cl}$ (halogen bonds) in **2**. Bond critical points (3, -1) are shown in blue, nuclear critical points (3, -3) – in pale brown, bond paths are shown as pale brown lines, length units – Å, and the color scale for the ELF and RDG maps is presented in a.u.

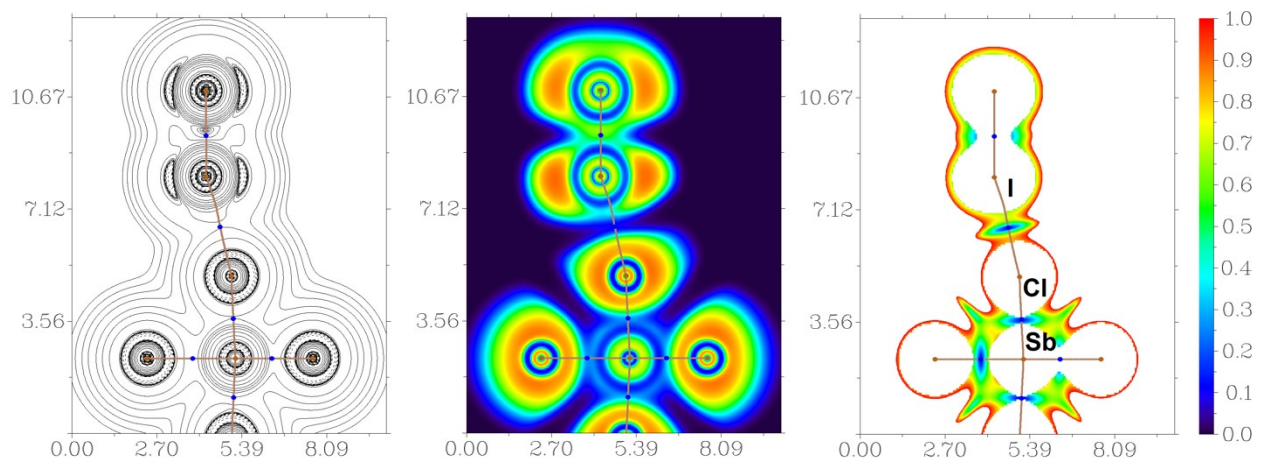


Figure S24. Contour line diagram of the Laplacian of electron density distribution $\nabla^2\rho(\mathbf{r})$, bond paths, and selected zero-flux surfaces (left panel), visualization of electron localization function (ELF, center panel) and reduced density gradient (RDG, right panel) analyses for intermolecular interactions $\text{I}\cdots\text{Cl}$ (halogen bonds) in **3**. Bond critical points (3, -1) are shown in blue, nuclear critical points (3, -3) – in pale brown, bond paths are shown as pale brown lines, length units – Å, and the color scale for the ELF and RDG maps is presented in a.u.

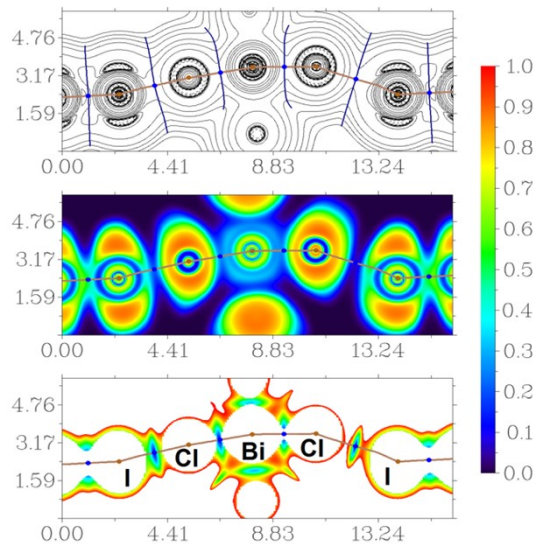


Figure S25. Contour line diagram of the Laplacian of electron density distribution $\nabla^2\rho(\mathbf{r})$, bond paths, and selected zero-flux surfaces (top panel), visualization of electron localization function (ELF, center panel) and reduced density gradient (RDG, bottom panel) analyses for intermolecular interactions (halogen bonds) $\text{I}\cdots\text{Cl}$ in **4**. Bond critical points $(3, -1)$ are shown in blue, nuclear critical points $(3, -3)$ – in pale brown, bond paths are shown as pale brown lines, length units – Å, and the color scale for the ELF and RDG maps is presented in a.u.

Table S15. Cartesian atomic coordinates for model supramolecular associates.

Atom	X	Y	Z
2			
Bi	5.752951	10.712625	7.070675
Cl	7.930878	10.712625	5.231822
Cl	3.718440	10.712625	8.689316
Cl	7.558773	10.712625	8.899267
Cl	5.725747	8.026184	7.195186
Cl	5.725747	13.399066	7.195186
Cl	4.194128	10.712625	4.634328
I	5.693686	4.929379	7.428619
I	5.693686	2.212371	7.428619
3			
Sb	8.885517	10.682325	3.961009
Cl	10.655451	10.682325	2.344544
Cl	11.044548	10.682325	5.766699
Cl	7.252226	10.682325	2.098870
Cl	9.103044	8.070710	3.910622
Cl	9.103044	13.293940	3.910622
I	9.862550	4.918570	4.284997
I	9.862550	2.202980	4.284997
4			
Bi	3.240988	6.537973	2.406044
Cl	2.999751	8.688656	3.950026
Cl	3.609017	4.241652	0.850706
Cl	0.580423	6.429025	2.371404
Cl	3.353911	7.924526	0.262899
Cl	5.908388	6.712064	2.878576
Cl	3.092115	5.118098	4.935531
I	8.837118	6.340856	3.480761
I	11.542799	6.191475	3.555350
I	-5.538482	6.340856	3.480761
I	-2.832801	6.191475	3.555350